

The Pennsylvania State University

The Graduate School

**TESTING CHANDELIER CELL ABNORMALITIES IN THE 16P11.2  
MICRODELETION MOUSE MODEL OF AUTISM SPECTRUM  
DISORDER**

A Thesis in

Biomedical Sciences

by

Alana A. Benn

© 2022 Alana A. Benn

Submitted in Partial Fulfillment  
of the Requirements  
for the Degree of

Master of Science

August 2022

The thesis of Alana A. Benn was reviewed and approved by the following:

Anirban Paul  
Assistant Professor of Neural and Behavioral Sciences  
Thesis Co-Advisor

Sergei Grigoryev  
Professor of Biochemistry and Molecular Biology  
Thesis Co-Advisor

Alistair Barber  
Professor of Ophthalmology, Cellular & Molecular Physiology,  
and Neural and Behavioral Sciences

Ralph Keil  
Associate Professor of Biochemistry and Molecular Biology  
Chair of Biomedical Science Program

## ABSTRACT

Autism spectrum disorders (ASD) describe a family of neurodevelopmental disorders that comprise a broad range of conditions such as abnormal reaction to sensory stimuli, deficits in social interaction and communication, as well as restricted and repetitive behaviors, interests, and activities. ASD has been diagnosed in more than 1% of children by 8 years in the United States. An observed male bias in development of ASD has been well noted whereas there is 4:1 male to female ratio of diagnosis. Onset of symptoms typically occurs early in childhood and may persist throughout life. The exact causation of ASD is unknown; however, numerous genes and environmental factors have been identified as contributing to the development of the disorder. Given its heterogeneous phenotypes and broad range in symptom severity across ASD patients, there is no standard treatment.

It is known that recurrent copy number variations (CNVs) in human 16p11.2 locus have been linked to neurodevelopmental and psychiatric conditions. Most notable, the microdeletion of 16p11.2 locus has been identified in individuals with obesity, developmental delays, and ASD. A plausible model for ASD proposes that genetic impairment and extrinsic insults converge on biological pathways that alter the function of cortical interneurons. Interneuron dysfunction may lead to impairment in synaptic transmission pathways which cause an imbalance in excitation/inhibition signaling that induce behavioral and cognitive deficits associated with ASD symptoms. Strikingly, the number of PV-expressing interneurons specifically chandelier cells (ChCs) have been shown to be reduced in the pre-frontal cortex (PFC) of individuals with ASD. However, since there are no specific cellular biomarkers for ChCs these rare neurons are inferred indirectly using combination of protein marker expression inclusion and exclusion criteria from immunohistochemical studies. Altogether, the prior

evidence suggests that the 16p11.2 microdeletion and a reduction in the number of chandelier cell bodies or stereotypic axon-initial segment (AIS) targeting boutons in general may be contributing risk factors in the development of ASD.

The broad goal of this thesis was to test the link between the 16p11.2 deletion and its impact on the ChCs in the pre-frontal cortex in a controlled experimental system, where these neurons were genetically labeled and therefore unambiguously tracked and reproducibly assayed. We hypothesized that mice harboring a deletion in chromosome 7 that is syntenic to the human 16p11.2 microdeletion may have altered counts and size distribution of AIS targeting boutons from the ChCs in the PFC as compared to the wild-type (WT) mouse. To test the hypothesis, a genetically engineered animal that harbors the heterozygous deletion in 16p11.2 ( $16p11.2^{\text{del}/+}$ ) was utilized. This  $16p11.2^{\text{del}/+}$  was bred to a triple transgenic Cre-driver, Flp driver, and a reporter line that specifically fluorescently labels ChCs. The aim of this thesis was to determine if there was an alteration in density and distribution of ChCs boutons that contact pyramidal neurons in the PFC. Tissue was coronally sectioned from mice, antibodies targeted against ChC boutons, AIS, and neuronal cell body were used to identify the contacts. Tissue images were acquired from super-resolution laser scanning confocal microscopy. The number and size of ChC boutons that contact the AIS of the pyramidal cell across different PFC regions were quantified using a fully automated image segmentation, object identification, registration and counting pipeline.

Overall, the thesis project demonstrated that there was a significant difference in the number of ChC boutons that actively innervate the AIS of PyNs in specific regions of the PFC between  $16p11.2^{\text{del}/+}$  experimental model and WT.

Data indicated that the number of ChC boutons that innervate the AIS of PyNs in the experimental model were reduced in the prelimbic cortex (PrL) as compared to the WT. Interesting prior mouse studies demonstrated that ChCs selectively connect to two distinct subsets of PyNs that occupy separate regions within the PrL region of the PFC. Most intriguing, reduction in ChCs were also noted within *in vivo* brain fMRI scans from human 16p11.2 microdeletion carriers. In addition, mice that harbor that syntenic deletion of human 16p11.2 with similar genetic deficiency both show reduced PFC connectivity, miswiring and long-range functional synchronization.

A significant reduction in ChC bouton innervation was also observed in the primary somatosensory region S1, but with a lower effect size. This is an interesting finding because it is well-known that human ASD patients have abnormal response to sensory stimuli, which has also been demonstrated in transgenic mouse models of ASD related genes which exhibit similar atypical behavior profile patterns when subjected to various stimuli. It has been established that functional deficits within the PrL and somatosensory cortices are associated with ASD behavioral and cognitive phenotypes. Notably, when the ChC bouton size on the AIS were analyzed, RegFS (designated as comprising the frontal primary somatosensory region) had increased ChC bouton size on the AIS in the 16p11.2<sup>del/+</sup> model.

These preliminary findings support existing human indirect immunostaining data from ASD patients and provide an impetus to further investigate how such changes occur during development in 16p11.2 microdeletion animals, as well as the impact it has on PrL and RegFS associated circuitry and behavior.

# TABLE OF CONTENTS

LIST OF FIGURES .....	vii
LIST OF TABLES .....	viii
ABBREVIATIONS .....	ix
ACKNOWLEDGEMENTS .....	x
CHAPTER 1: INTRODUCTION .....	1
1.1 Autism Spectrum Disorder Background .....	1
1.2 Autism: Genetic Associations .....	5
1.3 Autism: Brain Morphology and Connections .....	7
1.4 Autism: Cell Types and Circuits .....	10
1.5 Autism: Chandelier Cells .....	14
1.6 Autism: Mouse Models .....	17
1.7 Summary .....	21
CHAPTER 2: EFFECT OF 16p11.2 GENOMIC DELETION IN MICE WITHIN CHANDELIER CELLS.....	23
2.1 Theoretical Correlation Between ASD Associated Genes and Genes Within 16p11.2 Region .....	23
2.1.1 Human Phenotypes Associated with 16p11.2 Deletion.....	28
2.2 Thesis Introduction .....	30
2.3 Significance and Hypothesis .....	31
2.4 Materials and Methods .....	33
2.5 Results .....	37
2.5.1 Design of Data Analysis .....	37
2.5.2 Cell Number and Distribution .....	38
2.5.3 Chandelier Cell Bouton Size and Number of AIS Contact .....	45
CHAPTER 3: CONCLUSIONS .....	50
3.1 Discussion .....	50
3.2 Summary of Significant Findings .....	52
3.3 Future Directions .....	53
APPENDIX A: Tables of ROI and Mouse Atlas Images .....	55
APPENDIX B: Pipeline Workflow .....	59
REFERENCES .....	62

## LIST OF FIGURES

Figure 1.6.1a: Genes Mapped to Human 16p11.2 Conserved in Mice .....	20
Figure 1.6.1b: Schematic of Chromosome Engineering Strategy for 16p11.2 model .....	21
Figure 2.1.1: The Human 16p11.2 Locus .....	24
Figure 2.1.2: Genes in the Human 16p11.2 Region .....	25
Figure 2.5.2a: Summary of RFP Contacts on AISs Across all 8 PFC Regions (ANCOVA) .....	38
Figure 2.5.2 (b-e): Graphs of ANCOVA Analysis ChCs Boutons Contacts .....	39
Figure 2.5.2 (f-i): Graphs of ANCOVA Analysis ChCs Boutons Contacts .....	40
Figure 2.5.2j: Summary of RFP Contacts with GAT-1 on AISs Across all 8 PFC Regions (ANCOVA) .....	42
Figure 2.5.2 (k-n): Graphs of ANCOVA Analysis ChCs Boutons Contacts GAT-1 .....	43
Figure 2.5.2 (o-r): Graphs of ANCOVA Analysis ChCs Boutons Contacts GAT-1 .....	44
Figure 2.5.3a: Summary of RFP Contacts on AISs Across all 8 PFC Regions (ANOVA) .....	46
Figure 2.5.3b: Graph of RFP Contact_Area of RegFS .....	46
Figure 2.5.3c: Summary of RFP Contacts with GAT-1 on AISs Across all 8 PFC Regions (ANOVA) .....	48
Figure 2.5.3d: Graph of RFP Contact-with_GAT-1 Area RegFS .....	49
Figure A-1i: Mouse Coronal Sections Map (bregma 1.54 mm) .....	56
Figure A-1ii: Mouse Coronal Sections Map (bregma 1.10 mm) .....	58
Figure B-1i: Confocal Microscopy Channel Images .....	59
Figure B-1i: Example of Image Output of 4 Channels .....	60
Figure B-2: CellProfiler™ Image Identification Method .....	61

## LIST OF TABLES

Table 2.4.1: List of Materials Used .....	33
Table 2.5.2a: Summary Table of RFP Contacts on AISs Across all 8 PFC Regions (ANCOVA) .....	41
Table 2.5.2b: Summary Table of RFP Contacts with AISs GAT-1 all 8 PFC Regions (ANCOVA) .....	45
Table 2.5.3a: Summary Table of RFP Contacts on AISs Across all 8 PFC Regions (ANOVA) .....	47
Table 2.5.3b: Summary Table of RFP Contacts with GAT-1 on AISs all 8 PFC Regions (ANOVA) .....	49
Table A-1: Tables of ROI and Mouse Atlas Images .....	55
Table A-2i: Total Images Collected .....	58
Table A-2ii: Total Images Analyzed .....	58



## ABBREVIATIONS

Autism spectrum disorder	ASD
Axon initial segment	AIS
Chandelier Cells	ChCs
Copy number variation(s)	CNV(s)
Fast spiking interneurons	FSI
Medial ganglionic eminence	MGE
Parvalbumin	PV
Parvalbumin expressing positive	PV+
Pre-frontal cortex	PFC
Pre-optic area	PO
Pyramidal neurons	PyNs
Region of Interest	ROI

## ACKNOWLEDGEMENTS

Immeasurable appreciation and deepest gratitude are extended to everyone that has contributed to the completion of this thesis project in such a compressed timeline. This thesis project was a huge undertaking; it was an exercise in discipline, endurance, and perseverance; I am proud of all the preliminary data obtained. Given my steep neuroscience learning curve I was initially doubtful this could be achieved, but it was.

I want to thank each member of my thesis committee (Dr. Alistair Barber and Dr. Sergei Grigoryev) for offering their subject matter expertise, mentorship, and guidance for this thesis project. The conception, resources and completion of this project could not have been possible without the expertise of my thesis adviser and mentor Dr. Anirban Paul. Dr. Paul thank you for believing in my academic talents and lab skills, and most important providing me with the opportunity to continue my dream of completing advanced scientific study.

Immense thanks go to each member of the Paul lab who has assisted in this thesis project. Special thanks to Matthew Dickinson for his invaluable work in breeding and maintaining the mouse litters that were utilized for this project. Enormous gratitude goes to Mofida Abdelmageed doctoral candidate who is always willing to provide an explanation for my basic neuroscience questions. In addition, she was instrumental in assisting with lab work as well as providing moral support throughout the entirety of this thesis project.

Most important, I would like to give innumerable thanks to my family and friends that have provided me with encouragement, support, and love throughout this academic endeavor and beyond. Respect and gratitude to my ancestors who have paved the path for which I stand and walk along. And most of all, I give thanks to God for whom all is possible.

# CHAPTER 1: INTRODUCTION

## 1.1 Autism Spectrum Disorder Background

Neurodevelopmental disorders (NDDs) comprise a variety of conditions characterized by alterations in the development of the central nervous system (CNS). These alterations in the CNS manifest in varying symptoms such as aberrant behavioral patterns, as well as impaired cognitive processing, and motor development. NDDs often have overlapping symptoms which present in conditions that are categorized as intellectual disability (ID), learning disorders, communication disorders, motor disorders, attention deficit hyperactivity disorder (ADHD), autism spectrum disorder (ASD), epileptic encephalopathies (EE), and schizophrenia (SZ).<sup>1,2</sup> In particular, ASD has a global prevalence of 62 per 10,000 total affected and within the United States there has been a significant surge in prevalence whereas 1 in 59 (about 1%) of children are diagnosed by age 8.<sup>3,4</sup> Albeit statistical reports of incidence and prevalence of ASD are often confounded by the variability in biological and social determinants such as gender and sociodemographic status.<sup>5</sup> The implementation of more standardized early screening protocols, improved clinical assessment and overall societal recognition has added to an upsurge in identification of individuals with ASD.

The word autism is derived from the Greek word “autos” which signifies self, this term was coined in 1908 by Bleuler a psychiatrist to define the withdrawal from reality exhibited by schizophrenic patients.<sup>6</sup> In 1943 the psychiatrist Leo Kanner redefined the term autism as a diagnostic label describing early-onset symptoms observed in young children.<sup>7</sup> Kanner characterized autistic individuals with possessing deficits in language, performing repetitive and ritualistic behaviors as well as displaying disruptions in social and emotional relationships. Subsequently, in 1944 the clinician Hans Asperger identified children that shared most of the

Kanner autistic patterns except they lacked abnormalities in linguistics; this condition was then termed Asperger disorder.<sup>6</sup> Throughout the ensuing decades the diagnostics and classifications of autism have been scrutinized and delineated in standardized guidelines established in editions of the Diagnostic and Statistical Manual of Mental Disorders (DSM) by the American Psychiatric Association and the International Classification of Diseases (ICD) by the World Health Organization. Within the current revisions of DSM-V and ICD-10 autism disorder has evolved into an umbrella term ASD that encompasses several similar conditions: pervasive developmental disorders (PDDs): autistic disorder, Asperger's syndrome (AS), pervasive developmental disorder-not otherwise specified (PDD-NOS), and child disintegrative disorder.<sup>8,9</sup> Altogether ASD describes a family of neurodevelopmental disorders that comprise a broad range of symptoms such as abnormal reaction to sensory stimuli, deficits in social interaction and communication, as well as restricted and repetitive behaviors, interests, and activities.

ASD symptoms affect an individual throughout their lifespan, with an onset that typically manifests during early development prior to 3 years old. Since there is such variability in severity of the symptoms and overall heterogeneity in phenotypes across individuals with ASD, there is no universal biomarker for detection. Therefore, conventional diagnosis is performed by observing behaviors associated with the core ASD deficits. The current recommendations suggest screening for ASD with validated ratings and assessment scales for children 18 to 24 months by a trained pediatrician. While final diagnostics occurs after age 8 when typical developmental milestones are normally achieved by individuals.<sup>10</sup> Though symptoms are typically observed and diagnosed early in childhood, symptoms may present later in life once social stressors exceed the restricted range of functioning of an ASD individual.<sup>11</sup>

Most striking more than 70% of individuals with ASD also have other co-existing medical, psychiatric, or neurological conditions. Common co-morbidities are ADHD, anxiety, bipolar disorder, epilepsy, gastrointestinal problems, intellectual disabilities, motor abnormalities, neuroinflammation and immune disorders, obesity, schizophrenia, sleep disorders, Tourette syndrome and tic disorders.<sup>6,10</sup> Moreover co-morbidities such as neuroanatomical abnormalities, for example increased brain volume particularly in the cortical region of the frontal lobe have been well documented.<sup>12</sup> Additionally, dysmorphic features such as abnormal head size (typically macrocephaly) develop; however in some patients, microcephaly has also been assessed.<sup>13,14</sup>

Though sex bias is exhibited in many common diseases, in ASD cases there is a male preponderance whereas there is a 4:1 male to female ratio of development.<sup>11</sup> Plausible theories have been posited to explain this sex bias such as the notion that prenatal hormones in particular testosterone drive unfavorable genetic-environmental interactions “extreme male brain theory”, the second X-chromosome in females bestows gene protective effects, and the genetic liability hypothesis which suggests that females have a higher threshold for genetic mutations that affect ASD risk genes.<sup>15</sup> In a study by Zhang *et al.*, a mutational burden analysis was performed which evaluated *de novo* mutations in ASD risk genes from whole exome sequencing (WES) and whole genome sequencing (WGS) datasets of ASD and control groups.<sup>16</sup> Investigators found a higher prevalence of *de novo* mutations causing loss-of-function in the risk genes within females affected by ASD opposed to males, suggesting that females require a higher genetic mutational load for ASD diagnosis. Further studies surveying gender burden have found that in second-born male siblings the risk for developing ASD is three-fold higher than for female second-born siblings, thus emphasizing the increased penetrance of genes contributing to ASD in males.<sup>17</sup>

Although numerous intrinsic and extrinsic factors have been identified as contributing to the development of ASD, the exact causation is unknown. Intrinsic factors such as mutations in ASD risk genes can be inherited in the germline, can occur postnatally in somatic cells, or are modified by epigenetic processing have been extensively studied in pursuit of the etiological discovery of the disorder. Extrinsic factors such as exposure to environmental toxins *in utero*, pre-natal insults from pathogenic infection or maternal immune activation against the fetus as well as adverse peri-natal factors may also contribute to the disorder.<sup>6</sup> In addition, advanced parental age at conception especially increased paternal age has been shown to elevate the risk of offspring to develop ASD.<sup>18</sup> Notably, accumulating evidence has shown that disruptions in pathways that underly the microbiome-gut-brain axis and dysbiosis in the gut microbiome of both the mother and fetus may give rise to neurobehavioral and intestinal dysfunction in ASD patients.<sup>19,20</sup>

Given the constellation of symptoms associated with ASD it is a challenge to definitively diagnose and specifically treat the disorder. However, early diagnosis could improve long-term prognosis by finding the appropriate treatment strategy to manage an individual's symptoms. Current therapeutic options consist of both pharmacological and non-pharmacological interventions which only treat the symptoms. Treatments include but are not limited to following types of drugs: psychostimulants, atypical antipsychotics, antidepressants, NMDA receptor antagonists and anti-epileptics. ASD treatment regimens may include non-pharmacological interventions such as cognitive and social-behavioral therapies, herbal medicine, as well as nutritional and vitamin supplements. Overall, there is no unified model of causation, definitive biomarkers, or specific mode of transmission for ASD development. Altogether, ASD not only has a profound impact on the quality of life of the patient, but also on the caregivers and society

at large due to the substantial healthcare, societal resources and finances required to maintain an individual with ASD.

## **1.2 Autism: Genetic Associations**

Though ASD is multifactorial in causation, genetics contributes largely to the development and severity of the disorder. Epidemiological analyses surveying affected individuals (proband) in twins, single and multiplex siblings, as well as cohort studies (comparison of probands from different families) have provided evidence that ASD is heritable.<sup>21-23</sup> The seminal twin study conducted in 1977 by Folstein and Rutter asserted that there are genetic influences of ASD, the study examined individuals diagnosed based on ASD behavioral patterns since then numerous family studies like this were conducted globally.<sup>24</sup> Moreover, studies have indicated that a myriad of different symptoms with varying degrees of severity could be exhibited across family members and even amongst affected twins, thus differences in the accepted diagnostic guidelines such as DSM and ICD could not unambiguously discern if heritability is a factor. Updated meta-analyses that control for differences in methodological diagnosis of ASD behavior confirmed that the concordance rates of heritability of ASD development within affected monozygotic, dizygotic and siblings range from 50-90%, 0-30%, and 3-26%, respectively.<sup>17,25</sup>

The advent of more advanced molecular techniques such as high-resolution chromosomal microarray, and next generation sequencing technology has allowed for deciphering of chromosomal loci and discrete molecular signatures that are associated with ASD. Genome-wide association studies (GWAS) of patient cohorts versus controls in the population have identified genetic variations in allele frequency of less than 1% such as deletions, duplications, and insertions of one nucleotide that are single nucleotide polymorphisms or variations (SNPs or

SNVs). Moreover, whole exome sequencing (WES) and whole genome sequencing (WGS) in patient cohorts and ASD affected and non-affected families discovered larger structural variants such as copy number variants (CNVs) and non-coding loci within the genome that are associated with disease risk.<sup>26</sup> In addition, genetic variations that occupy the genome of ASD individuals may occur as common or rare events and the mode of transmission can be inherited via *de novo* germ-line or post-zygotic mosaic cellular development.<sup>27,28</sup> Overall, the precision of advanced molecular techniques have allowed the discernment of patterns of genetic liability that drive ASD phenotypic expression.

Numerous ASD focused genetic databases and patient specimen repositories such as Simons Foundation Autism Research Initiative (SFARI) and Simons Powering Autism Research for Knowledge (SPARK) have curated datasets and identified over 1000 genes associated with the development of ASD.<sup>2,29</sup> However, many of these ASD risk genes are linked to the development of other NDDs also. To date no specific mutation has been identified which is uniquely associated with the development of ASD only. The consolidation of data taken from ASD patient genomic and exome studies, *in vivo* animal models, and *in vitro* tissue culture have indicated that genes that contribute to ASD participate in a variety of biological functions with converge on specific aspects. Biological pathways that are involved in brain development and function in particular the cortex region, synapse function, transcription and translational regulation, as well as chromatin remodeling.<sup>10</sup> More recent studies have expanded that list to encompass genes that are implicated in microglial activation, axonal outgrowth, cytoskeletal and vesicle machinery which are associated with synaptic signaling.<sup>30</sup>

Though the occurrence of CNVs in ASD is about 1%, they have a high penetrance as compared to the other genetic variations.<sup>31</sup> CNVs are a class of unbalanced structural variants



that are characterized by deletions, and duplications of DNA sequences which may decrease, increase, or have a neutral phenotypic impact. The size of CNVs range from 50 base pairs to 5 mega base pairs, and the large effect size can occupy multiple regulatory, intragenic, intronic regions which may endow pleiotropic effects.<sup>32</sup> CNVs derive from non-allelic homologous recombination (NAHR) between low-copy repeat (LCR) sequences. Hence these non-allelic pairing of sequences and chromosomal translocations may cause the occurrence of deletions, duplications and inversions in chromosomal loci.<sup>32</sup> The pattern of CNV formation can either be recurrent whereas the same size and genomic content is common across related and unrelated individuals or nonrecurrent which describes unique size and genomic content at a given position in unrelated individuals. Further, CNVs range in size which allows for dosage-sensitive genes to be incorporated within or adjacent to the region and ultimately cause reciprocal change in phenotypic expression depending on the loss-or-gain of sequences within the region.

ASD is sub-classified into two types syndromic and non-syndromic (also known as idiopathic) as prescribed by clinical criteria. Syndromic refers to conditions that have neurobehavioral phenotypes and/or dysmorphic features that are associated with known disorders that are result of single gene mutations, small CNVs, chromosome abnormalities.<sup>33</sup> Idiopathic describes neurobehavioral phenotypes with or without dysmorphic features which develop from an unknown etiology. Identification of targeted mutations that produce this known syndromic trait has provided scientist with good models to test for ASD due to having targeting regions that produce these phenotypes.

### **1.3 Autism: Morphology and Connections**

Examination of gross brain structure and tissue through physical assessment and brain imaging technology has demonstrated that there are abnormalities in the structure and tissue of

individuals with ASD as compared to neurotypical individuals. Results from neuroanatomical studies have indicated that sub-sets of ASD individuals exhibit microcephaly at birth and accelerated growth in brain circumference by the age of 2 years, while other sub-sets present with normal brain growth.<sup>30</sup> Moreover, other structural studies employing magnetic resonance imaging (MRI) have demonstrated neuroanatomical differences between controls and ASD patients in total brain volume, cortical gray and white matter volume mainly (frontal, temporal, and cingulate cortices), extra-axial cerebral spinal fluid volume, and amygdala volume.<sup>30</sup> Furthermore, functional MRI (fMRI) is a technique that measures changes in blood-oxygen level-dependent (BOLD) contrast in images due to body motion has been utilized in numerous studies to distinguish differences in neuronal signaling activity. These studies have revealed that there are deficits in visual processing, executive function, language, and basic and complex social processing skills in ASD.<sup>34</sup>

Brain abnormalities within the cerebral prefrontal cortex; limbic system structures, including the hippocampal formation and amygdala; basal ganglia; thalamus; brainstem; and cerebellum have been identified in ASD.<sup>35</sup> In a study by Bedford *et al.*, neuroimaging was obtained from a total of 1,327 ASD-affected and controls; these results indicate that there is greater cortical thickness in patients within the superior temporal gyrus and inferior frontal sulcus. In addition, greater thickness in specific regions correlated with gender and youth as well as the severity of clinical ASD symptoms and full-scale intelligent quotient (IQ).<sup>36</sup> Although neuroanatomical evaluation may be influenced by confounding factors such as age, sex, and variability in technical assessment, it is widely accepted that there are neuroanatomical differences between healthy and ASD affected individuals.

Postmortem studies conducted on autistic brains have provided evidence that not only neuroanatomical, but also cellular morphology, distribution, and overall cellular circuitry are considerably altered by ASD. Alterations such as reduction in cell size and increase in cellular density can be observed across all ages within their hippocampus, limbic system, entorhinal cortex, and amygdala.<sup>37</sup> ASD-related brain defects such as dysplasia, altered neurogenesis, neuronal immaturity, and abnormal neuronal migration resulting in focal deformation in the cytoarchitecture can be identified across the aforementioned brain regions. Other ASD related cellular defect such as heterotopia (mislocalization of neurons), reduction in Reelin protein required for neuronal migration during cortical lamination and increased neuropil (intercellular space comprised of dendrites, non-myelinated axons, synapses, glial and vasculature) in the frontal polar region and anterior cingulate gyrus emphasize ASD impacts early development.<sup>37</sup>

The elaborate organization of the human brain is exemplified by inter and intra-regional structural and functional connectivity. Structural connectivity describes the anatomical arrangement of the fiber tracts within the brain, while functional connectivity denotes a time between electrophysiological activity and de-oxygenated blood levels in distinct areas of the brain. Neural activity can be assayed for structural integrity by measuring changes in post-synaptic potential and dendritic currents of neural populations via electro and magnetoencephalography (EEG and MEG).<sup>38</sup> Functional connectivity can be tested by correlation of changes in metabolic demand in the brain with BOLD.

Connectivity refers to either the local signaling within a region for instance posterior cingulate cortex (PCC) or the global signal interaction between regions such as the PCC and the medial prefrontal cortex (mPFC).<sup>34</sup> Moreover, accumulating evidence has indicated that ASD perturbs neural connections both locally and globally. Aberrations in neural connections may be

described as either hypoconnectivity, which is an under or low connection relative to the standard neurotypical signaling or hyperconnectivity that is an increased or stronger signaling. Conflicting resting-state fMRI studies have found patterns of both hypo and hyper connectivity in subsets of ASD patients, such confounding results may be due to bias in gender, age, or severity of symptoms. In a resting-state fMRI study by Haghighat *et al.*, the controls (typically developing) and ASD individuals were matched based on age, full IQ, and gender. The study results indicated that hyperconnectivity occurs during childhood for ASD and both hypo- and hyperconnectivity exist after childhood signifying neural connection impairment in persistent.<sup>39</sup>

#### **1.4 Autism: Cell Types and Circuits**

Of particular interest, is the cortical region of the brain because alterations in cortical domains associated with cognitive, sensory, and social perception have been associated with ASD behavioral deficits. The mammalian cerebral cortex is the outermost layer of the brain which consists of four lobes: frontal, parietal, temporal, and occipital. Moreover, the cortex can be further characterized by three types of functional areas: sensory, motor, and association areas. Further, the cortex is intricately comprised of hundreds of neuronal cell types and a variety of glia that characterize the grey matter. The cortex tissue is organized into six layers designated as I to VI, these layers develop via a stereotyped “inside to out” pattern of development whereas the deepest layers emerge first and superficial last.

The two major neuronal cell types that reside in the cortex are projection neurons (PN) also referred to as principal cells and interneurons (IN). Projection neurons have axons that extend to distant intracortical, subcortical, and sub-cerebral targets. The predominant projection neuron type in the cerebral cortex is the pyramidal neuron cell (PyN) which is a glutamatergic excitatory neuron.<sup>40</sup> PyNs are generally dispersed throughout layers II to VI. The name

pyramidal reflects the cellular morphology of the triangular-shaped soma as well as elongated apical and short clustered basal dendritic branches. The dendritic spines of PyNs are the main postsynaptic element of all cortical excitatory synapses. PyNs are commonly classified according to their axonal projection site, where they are involved in different synaptic circuits, thus endowing them with diverse functions. In general, glutamatergic neurons are born in the ventricular zone of the embryonic pallium and they migrate radially towards the pia mater to construct the neuronal layers.

Cortical interneurons have neurites that make local connections, thus confining their axon and dendritic arbors to the cortex. Though the majority are  $\gamma$ -aminobutyric-acid-releasing (GABAergic) inhibitory neurons, a small population function as excitatory.<sup>41</sup> Unlike cortical neuronal and non-neuronal cell types, cortical interneurons development entails a series of critical milestones over a protracted trajectory. GABAergic interneurons are produced from progenitor cells in the ventricular zones of the dorsal pallium and the ventral ganglionic eminences (sub-pallium).<sup>42</sup> Post-mitotic interneurons endure a long tangential migration through several characterized streams towards the cortical plate.<sup>43</sup> Ultimately, interneurons establish final locations within a cortical region and layer stereotypical for their sub-type.

Cortical interneurons are categorized by their morphology, biochemical markers, electric signals, molecular signatures and the subdomain of the neuron (axon, dendritic, or soma) they target. Cortical interneurons are broadly sub-divided into the following groups basket cells (large, small, or nest basket cells); chandelier cells (ChCs); Martinotti cells; bipolar cells; double bouquet cells; bitufted cells; neurogliaform cells; and layer I interneurons and excitatory spiny stellate cells.<sup>41</sup> Critical to interneurons function is their expression of specific neuropeptide markers such as  $\text{Ca}^{+2}$ -binding protein parvalbumin (PV), the neuropeptide somatostatin (SST),

and the ionotropic serotonin receptor 5HT3a (5HT3aR), Vasoactive intestinal polypeptide (VIP), neuropeptide Y (NPY), and cholecystokinin (CCK) and the Ca<sup>+2</sup>-binding proteins calretinin (CR) and calbindin (CB).<sup>44</sup> The three main groups of interneurons are: PV-expressing basket and chandelier neurons; SST-expressing neurons; and 5HT3aR expressing neurons which account for about 100% of GABAergic interneurons in somatosensory cortex.<sup>44</sup>

The diverse functional capacity of the brain relies upon the elaborate cytoarchitecture of each cell as well as the hierarchical formation of intricate cellular circuitry across the brain.

A circuit can be defined as a set of interconnected components that combine to fulfill a specific function. Neural circuits can describe a cluster of neurons that receive electrochemical information to modify and transmit to other neuron clusters or it may consist of a network of interconnected brain regions that integrate information and perform the consolidated task.

The formation development of neuronal circuitry occurs in sequential steps and throughout this process the developing brain circuits are both active and functional to carry out spontaneous tasks.<sup>45</sup> After GABAergic or glutamatergic neurons localize to their final position, they form proto-ensembles (the initial group of co-active neurons that produce subsequent ensembles) that are joined by gap junctions which form electrical synapses.<sup>42</sup> Next, the electrical synapses are replaced by chemical synapses and developmental apoptosis elimination damaged cells.

Throughout the formation of neural circuitry internal inputs from other precursor neuronal cells and non-neuronal cells aid the synaptic formation, while the final step of neural connection refinement is also influenced by extrinsic factors.

GABAergic interneurons target neuronal sub-domains (soma, axon, dendrites) and thus regulate spatiotemporal activity of projection neurons in varying degrees based on the location of innervation. Moreover, GABAergic interneurons modulate the timing of pyramidal cell firing,

coordinating network activity as well as producing cortical patterns. In addition, studies have indicated that GABAergic interneurons elevate the dynamic range of cortical circuitry, control sensory receptive fields and plasticity and react to dynamic modifications in excitation signals.<sup>44</sup> Disruption in neuronal circuitry has been linked with the development of several neurological disease such as epilepsy, schizophrenia, anxiety disorders and ASD.<sup>44</sup> One plausible explanation for autism proposes that altered function of cortical interneurons are the likely cause of synaptic excitation/inhibition (E/I) imbalance in the cerebral cortex in autism, whereas hyperexcitability, increased spiking and cortical circuitry noise induce ASD symptoms.<sup>46</sup> This theory supports an increase in excitatory signaling which partially explains co-morbidities such as seizures which are induced by excitatory signaling; however, this symptom occurs only in a small subset of ASD. Overall, numerous neuronal cell types and sub-types are involved in controlling (E/I) balance and each type produces distinct neurotransmission given the context of the brain state.

As examined on a macroscopic level, the brain structure of an ASD patient may exhibit extreme or negligible alterations which may or may not coincide with the severity of the symptoms. The brain contains hundreds of distinct cell types and each display discrete morphology, produce specific proteins, and harbor distinct molecular signatures, thus it stands to reason that disruption at the cellular level may play a critical role in neural dysfunction. For example, impairment of dopaminergic neurons within the substantia nigra are substantial to produce symptoms of Parkinson's disease, and restoration of cellular dopamine levels is a common treatment for idiopathic Parkinson's disease. Overall, each GABAergic interneuron subtype has a distinct response to neuromodulators, actions that critically impact the function of neocortical circuits and are concomitant with changes in brain states and behavioral patterns.<sup>44</sup>

A study by Velmeshev *et al.*, assessed cell-type specific mechanisms of ASD by performing single-cell nuclei RNA sequencing on post-mortem brain tissue collected from ASD patients and neurotypical controls, and then compared these results to an ASD reference database. Investigators found that in patients there was differential expression of ASD associated genes across 4 frontal and temporal cortex region that converge on pathways linked to immune response.<sup>47</sup> Most striking in patients, alternate splice forms of genes were found enriched for genes related to synaptic function that are preferentially expressed in adult interneurons and neurons.<sup>47</sup> Moreover, an ASD high-risk gene *CH8* and a master-regulator of other ASD-related genes during development were identified as hypomethylated in the PFC of patients.<sup>47</sup> Taken together these results indicate that dysregulation of specific ASD related genes can be found in specific tissue and cell types in ASD.

## **1.5 Chandelier Cells**

The most remarkable GABAergic interneurons known to the mammalian brain are ChCs, they were identified in the 1970s by Szentagothai, and independently, by Jones.<sup>48,49</sup> As designated by their name, ChCs have a distinct morphology that resembles a candelabrum. ChCs have extensively branched axonal arbors referred to as cartridges which terminate in parallel arrays consisting of short vertical strings of presynaptic boutons that contact the axonic subdomains. More specifically, axons of ChCs selectively innervate the axon initial segment (AIS) of PyN; this subcellular region is responsible for initiating action potentials (APs) and maintains the polarity of the neuron. Accumulating evidence has demonstrated that alteration in ChC cartridge/bouton number and dysfunction in ChC connectivity are associated with neurological disorders associated with improper E/I imbalance such as schizophrenia epilepsy and ASD.<sup>50-52</sup>



Although ChCs are most abundant in cortical layers 2 and 3, they can also be found dispersed throughout all other cortical layers.<sup>49</sup> Outside of the neocortex, ChCs have been identified as occupying the piriform cortex, the dentate gyrus, hippocampus, and amygdala.<sup>49</sup> While in total inhibitory interneurons comprise only ~20% of cortical neurons, ChCs cells are the rarest in that they comprise less than 1% of the cortical inhibitory neuron population. Although *en masse* the ChCs represent a minority of the cortical interneurons, what makes them so powerful is that a single ChC can innervate hundreds of PyNs and potentially control the excitatory signal output. The geometry of a single ChC allows its cartridges to align with the AISs of PyNs and on average 3-5 boutons will have contacts.<sup>53</sup> Though the actual innervation of the ChC cell varies depending on laminar localization, region of cortex, and age of the animal.

Recently genetic markers that are involved in the formation of connections between ChCs and the AISs of PyNs have been ascertained. Receptor tyrosine kinase Erb4 a protein expressed by all PV<sup>+</sup> interneurons was the first molecule identified as being involved in ChCs bouton morphogenesis. Investigators testing *Erb4* conditional knockout mice found that ChC bouton density decreased even though ChC cartridge density, length and overall morphology were not altered.<sup>54</sup> In a concomitant study by Tai *et al.*, the role of Erb4 in ChC morphogenesis was linked to Deducator Of Cytokinesis 7 (DOCK7) that functions as a cytoplasmic activator of Erb4 that stimulates ChC cartridge and bouton development. Investigators found that knockdown of *DOCK7* in the neocortex of mice reduced the size and density of ChC boutons and caused disorganization in ChC cartridge connections.<sup>55</sup> Accordingly, the ectopic rescue of *DOCK7* expression significantly increased ChC bouton density and size.<sup>55</sup>

ChCs and basket cells are the two major sub-types of PV expressing cells that are associated with a fast-spiking (FS) neural AP firing pattern. In particular, FS interneurons (FSI)

fire at a steady-state continuous high frequency of greater than 50 Hz; this is substantially higher than the firing rate of the principal cells in which FSI targets.<sup>56</sup> Moreover, FSI can sustain a series of brief APs with the large and fast after hyperpolarization phases (refers to phase that the cell's membrane potential falls below normal resting potential and minimal spike frequency adaptation (negligible adjustment of firing rate to constant stimuli)).<sup>44</sup> In addition, FSI has the lowest input resistance (more open channels) and fastest membrane time constant (time to repolarize).<sup>44</sup> Taken altogether, these features of FSI contribute to their ability to produce fast synaptic responses. Even though ChCs and basket cells are both PV expressing FSI, there are clear distinctions in their electrophysiology which contribute to how each coordinate and control cortical neurons neurotransmissions.

Cortical interneurons develop in waves whereas each interneuron sub-type follows a distinct schedule of stages. The developmental trajectory of cortical interneurons follows these important sequential stages: birth (post-mitotic, migration, axonal guidance, dendritic arborization, synaptic formation, and maturation {pruning}). Primarily, GABAergic interneurons derive from a select transcription factor expressing progenitor cells (PCs) located in either the medial ganglionic eminence (MGE) and the adjoining preoptic area (POA), or caudal ganglionic eminence (CGE). In particular, PV and SST expressing interneurons originate from Nkx2.1 homeodomain transcription factor expressing PCs located in the MGE-POA region. Various studies in mice employing NKx2.1 Cre-lines in fate-mapping, *in utero* retroviral injections in MGE and MGE transplantation into the neocortex have verified that most or all ChCs originate in the MGE and adjoining POA.<sup>52</sup> Moreover, the genesis of ChCs begins at embryonic day embryonic day (E)12 and their peak birth wave occurs between E 16-17.<sup>52</sup> PV

expressing interneurons are generated later than other sub-types such as SST which are all born by E 14.5 and most striking ChCs are the latest born of all interneuron sub-types thus far.

## **1.6 Autism Mouse Models**

ASD is a complex disorder with heterogeneous symptoms that overlap with other NDDs, and there are no standard biomarkers for detection; therefore, the accepted means of diagnosis is through behavioral observations. Deficits in core symptoms clustered in domains for social interaction as well as restricted and repetitive patterns are coordinated or controlled by areas within the prefrontal cortex which is highly developed in the human brain unlike other mammals.<sup>12,57</sup> Humans exquisitely exhibit specialized social cognition, emotions, and perform the theory of mind tasks in a manner that does not occur in other mammals and is not inherent to non-human primates.<sup>57</sup> Moreover, ASD is a distinctively human disorder thus the full spectrum of behavior symptoms cannot be reliably reproduced in animal models.<sup>58</sup> Since ASD is a multifactorial disease, animal models are employed to demonstrate specific phenotypes that are related to the neurological insults induced by genetic engineering, epigenetic manipulation, or extrinsic agents rather than completely recapitulate ASD. In general, animal models provide a tractable system to test the effects of specific ASD risk related factors on neuroanatomy and histology, neural circuitry, and behavior outcomes.

Other experimental systems, such as *in vitro* models, can provide biologically significant information about cellular structure, protein-protein interactions, and the functionality of molecular machinery. In a study by Zaslavsky, K. *et al.*, human induced pluripotent stem cells (hiPSCs) differentiated into neural-like cell lines derived from either ASD patient tissue or gene-edited neurotypical tissue were developed to survey the effects of ASD risk gene *SHANK2*.<sup>59</sup> Result demonstrated that loss of *SHANK2* altered expression of genes that function in neuronal

formation and promoted hyperconnectivity of neural circuitry.<sup>59</sup> Urresti, J. *et al.*, employed patient derived tissue harboring either 16p11.2 reciprocal CNVs to generate cerebral organoids that recapitulate 3-dimensional cytoarchitecture to measure cortical volume and survey transcriptomic expression and proteomic levels for genes in active during early neurodevelopment.<sup>60</sup> Results showed that 16p11.2 reciprocal CNVs caused alterations in cortical size and dysregulated genes that function in neuronal migration, and synaptic pathways.<sup>60</sup>

Animal models are the best systems to explore physiological processes experimentally and to some extent provide clinically relevant outputs. There are numerous animal models that scale from low complexity invertebrates to high complexity vertebrates which are employed in ASD research. Even though *Drosophila melanogaster* (fruit fly) and *Danio rerio* (zebrafish) exhibit low anatomic conservation to humans their genomes harbor numerous gene homologs. A study modelling 16p11.2 deletion in fruit fly RNAi lines identified neurodevelopmental phenotypes that were caused by the interplay between specific genes within that microdeletion.<sup>61</sup> In zebrafish several genes homologous with the 16p11.2 genomic region were found to have dosage effect on phenotypic expression of features produced in early brain development.<sup>62</sup> In general all these animals of lower anatomical complexity serve as good systems to test biologically relevant molecular and protein interactions.

Non-human primates are superb systems to model ASD phenotypes, however, the cost and expertise of maintenance, as well as ethical considerations with genetic manipulations minimize their utility. Of all the small mammals that are currently employed in research, rodents are the most frequently used due to their low maintenance, high reproducibility, length of lifespan, and most important ease to genetically modify. However, rats provide a better readout

for behavioral testing than mice because rats exert more social motivation.<sup>63</sup> Mice are commonly used for human genetic research because 90% of the mouse genome map is orthologous to the human genome therefore, a high degree of genetic conservation exists between the organisms.<sup>64</sup>

There are 3 commonly utilized mouse models of 16p11.2 CNV. The Mills lab generated reciprocal CNV mouse lines 16p11.2<sup>del/+</sup> or 16p11.2<sup>dp/+</sup> (16p11.2 duplication) from mouse chromosome 7 position F4 region (Slx1b-Sept1) which is syntenic to human 16p11.2 locus. Refer to figure 1.6.1a illustrating human gene within 16p11.2 which are conserved in mouse chromosome 7. The Dolmetsch lab utilized mouse chromosome 7 and generated the deletion of the Coro1a-Spn gene interval and the Herauld lab generated 16p11.2 mice from the deletion/duplication of the Sult1a1-Spn genetic interval of mouse chromosome 7.<sup>65</sup> All three mouse lines exhibited social and cognitive deficits as assessed by various behavioral paradigm testing.

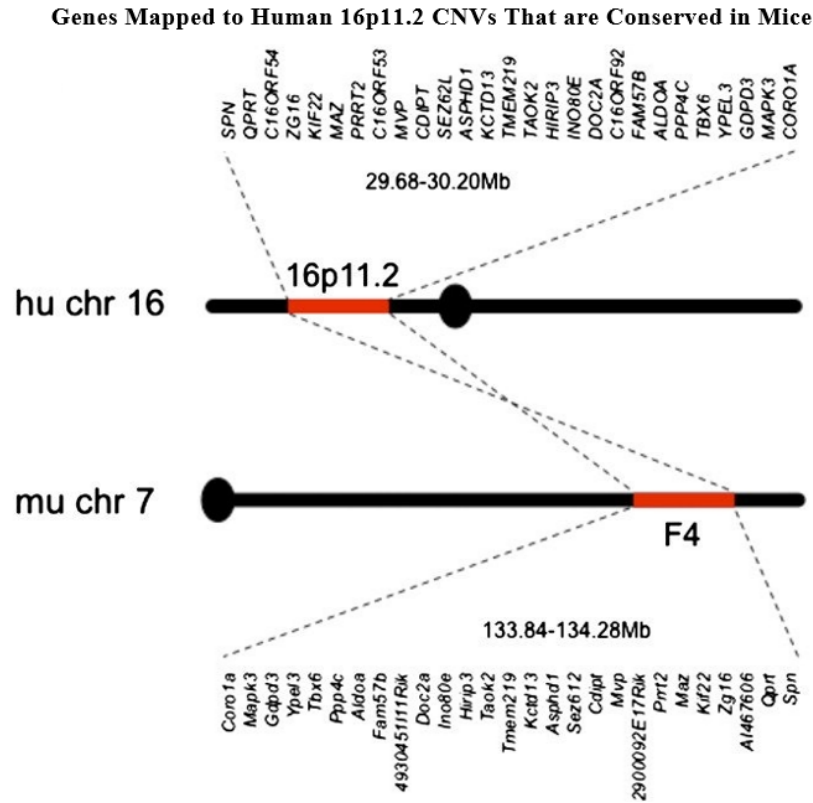
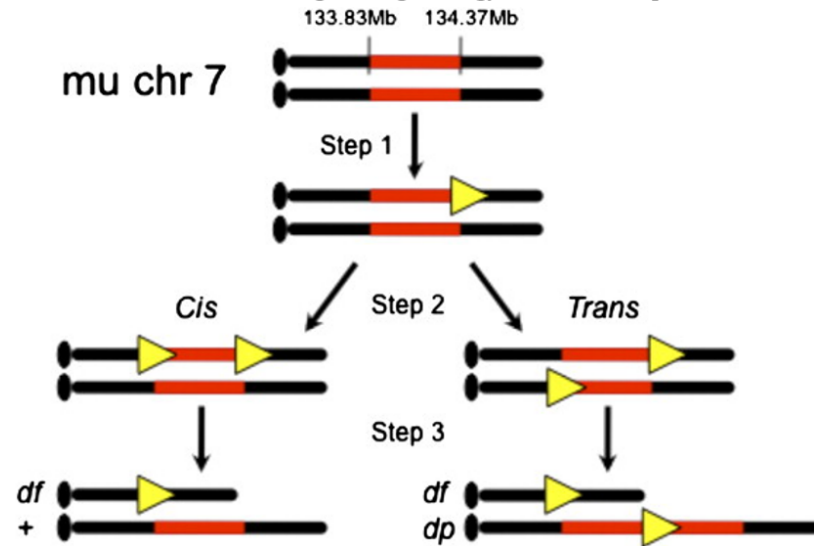


**Figure 1.6.1a:** Generation of 16p11.2 reciprocal CNV models, the diagram illustrates the genes mapped to human 16p11.2 CNVs that are conserved in mouse

In this thesis project the 16p11<sup>del/+</sup> mouse line generated by the Mills lab was utilized. The generation of the mouse line was described in the paper by Horev *et al.*, whereas chromosome engineered mouse models harboring either a deletion or duplication in orthologous chromosome 7 loci to human 16p11.2 were studied.<sup>66</sup> Refer to figure 1.6.1b which depicts the generation of the 16p11.2 mouse model. The investigators found that the mouse models had dosage-dependent changes in expression, viability, brain structure and behavior, most important the deletion model had more severe neurological phenotypes than the duplication. Further evaluation of the 16p11.2<sup>del/+</sup> indicated that the litter size was smaller than expected and underrepresented as compared to the 16p11.2<sup>dp/+</sup> litter. In addition, 16p11.2<sup>del/+</sup> mouse lines demonstrated low post-natal survival rate. Notably mice that harbor a homozygous deletion in 16p11.2 are not viable.

### Schematic of Chromosome Engineering Strategy to Generate 16p11.2 Models



Source: adapted from Horev G. *et al.*, PNAS (2011)

**Figure 1.6.1b:** The diagram illustrates the schematic of the chromosome engineering strategy used to generate mouse models of 16p11.2 reciprocal CNVs

## 1.7 Summary

Autism spectrum disorders (ASD) describe a family of neurodevelopmental disorders that comprise a broad range (spectrum) of symptoms such as abnormal reaction to sensory stimuli, deficits in social interaction and communication, as well as restricted and repetitive behaviors, interests, and activities. The exact causation of ASD is unknown; however, numerous genes and environmental factors have been identified as contributing to the development of the disorder. It is known that recurrent copy number variations (CNVs) in human 16p11.2 locus have been linked to neurodevelopmental and psychiatric conditions. Most notable, the microdeletion of 16p11.2 has been identified in individuals with obesity, developmental delays, and ASD. A plausible model for autism proposes that altered function of cortical interneurons are the likely cause of synaptic excitation/inhibition imbalance in the cerebral cortex in autism, whereas hyperexcitability, increased spiking and cortical circuitry noise induce ASD symptoms.

Moreover, the number of PV-expressing interneurons specifically chandelier cells (ChCs) have been shown to be reduced in the pre-frontal cortex of individuals with ASD. However, since there are no specific cellular biomarkers for ChCs these rare neurons are inferred indirectly using inclusion and exclusion criteria from immunohistochemical studies. Taken together, the prior evidence suggests that the microdeletion of 16p11.2 and a reduction in the number of ChCs may be contributing risk factors in the development of ASD.

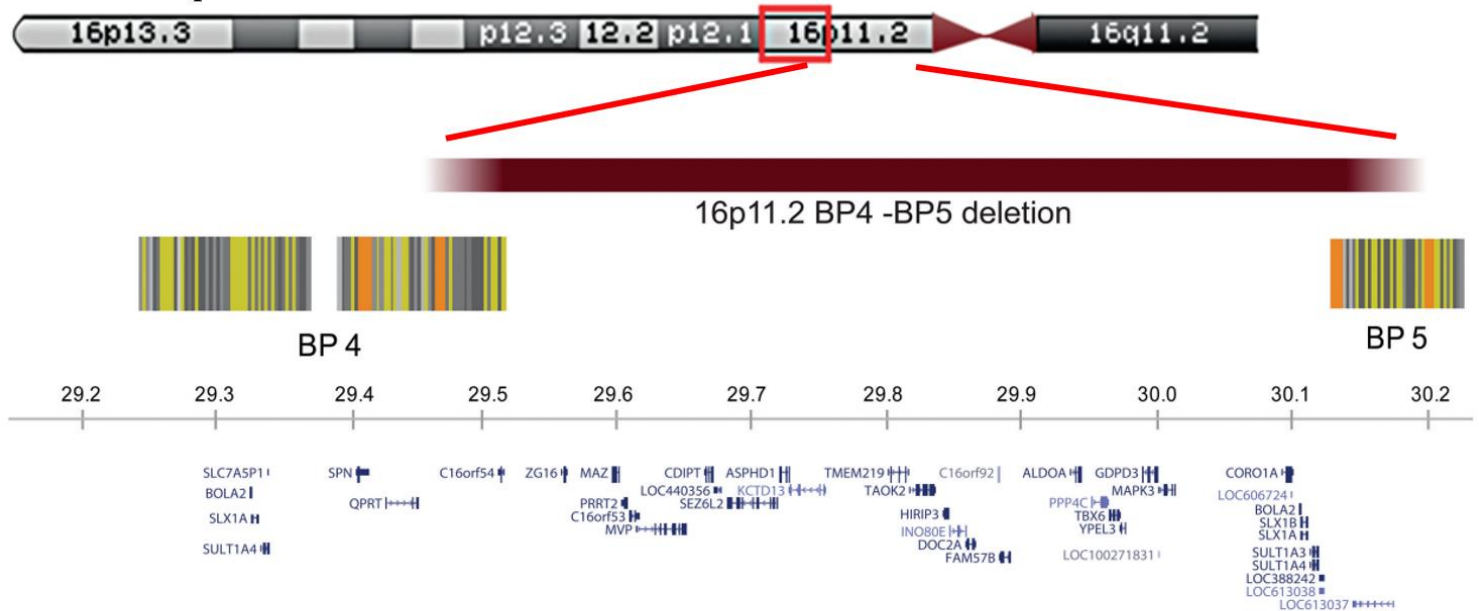


## **CHAPTER 2: EFFECT OF 16P11.2 GENOMIC DELETION IN MICE WITHIN CHANDELIER CELLS**

### **2.1. Theoretical correlation between ASD associated genes and genes within 16p11.2 region**

Located on the proximal arm of chromosome 16, the human gene locus 16p11.2 (chromosome 16, position 11.2) spans a region 500-600 kb and encompasses 27-29 genes. Refer to figure 2.1.1 which depicts the human 16p11.2 locus. The genomic position is flanked on either side by LCR sequences and demarcated by BP4 and BP5 at genomic sequence coordinates of approximately 29.5 and 30.1 Mb.<sup>65</sup> Reciprocal deletions and duplications of 16p11.2 CNV have been observed in the general population at rates of  $\geq 0.043$  and  $\geq 0.053\%$ , respectively, while the frequency of the extremely rare triplication is unknown.<sup>67</sup> Moreover, 16p11.2 CNVs have been reported as one of the most frequent structural variants associated with NDDs and contribute to 1% of all cases of ASD. In fact, carriers of the deletion have a 38-fold increased risk of development of ASD, while the duplication carries a 20-fold increased risk.<sup>68</sup> Finally, epidemiological studies indicate that both the deletion and duplication of 16p11.2 CNV occur predominately through *de novo* events rather than inherited and evidence suggests that the pattern of inheritance for these reciprocal CNVs is preferentially maternal.<sup>67</sup>

## The Human 16p11.2 Locus

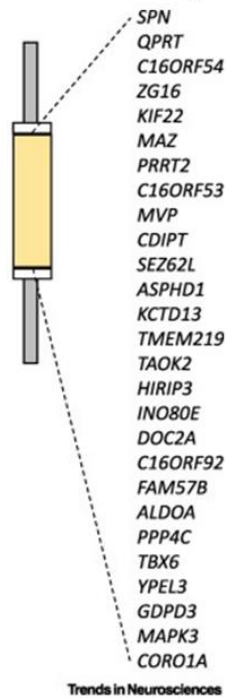


Source: adapted from Zufferey F. et al., J. Medical Genetics (2012)

**Figure 2.1.1:** The Human 16p11.2 Locus (human genome build hg18/NCBI 36)

As aforementioned there are 29 genes identified within 16p11.2 locus, these genes have been associated with biological pathways such as cell cycle progression and transcriptional regulation, as well as brain development and function. Refer to figure 2.1.2 denoting the 27 genes within the human 16p11.2 locus. Crepel *et al.*, conducted the first clinical study of 16p11.2 deletion associated with ASD and ASD traits in a three-generation family whereas none of the family members harbored other pathogenic CNVs within their genomes.<sup>69</sup> The investigators identified a deleted 118 kb region common to all affected and unaffected carriers of the 16p11.2 deletion; this narrow region consists of five genes: *MVP*, *CDIPT1*, *SEZ6L2*, *ASPHD1*, and *KCTD13*.<sup>69</sup> Notably, all offspring of the unaffected carrier that harbored the narrow deletion were formally diagnosed with ASD.<sup>69</sup> Though *MVP* and *SEZ6L2* were previously identified as candidate genes for ASD risk, all five genes are conspicuously expressed in the brain and involved in integral cellular functions.

### Genes in the human 16p11.2 region



Source: adapted from Rein B. *et al.*, Trends in Neurosciences (2020)

**Figure 2.1.2:** Genes in the human 16p11.2 region

Primarily, *MVP* encodes the major vault protein which is a key component of the vault cellular ribonucleoparticles. MVP functions in nucleocytoplasmic transport and is expressed across the nucleus–neurite axis in cerebrocortical and corticostriatal neurons.<sup>69</sup> Most interesting, MVP is involved in critical signaling cascades such as facilitating the nuclear import of tumor-suppressor molecule PTEN as well as mediating nuclear translocation and phosphorylation of STAT1.<sup>70</sup> Strikingly, alterations in PTEN are associated with macrocephaly and loss of PTEN has been implicated in neurobehavioral deficits including those manifested in ASD phenotypes.<sup>71</sup> The *SEZ6L2* gene encodes the seizure related 6 homolog-like 2 protein which is localized on the cell surface and during mouse and human embryonic brain development its expression is enriched in the CNS.

Notably, channel tetramerization domain containing 13 (*KCTD13*) is a high-risk gene for ASD that encodes an adaptor protein for Cullin 3 a core component of E3 ubiquitin ligase complex which mediates ubiquitination and degradation of Ras homology family member (RHOA) and other protein substrates. Though mutations in *KCTD13* have not been identified in human cases of ASD, studies from *ktcd13* gene knockout mouse models have demonstrated a reduction in synaptic transmission that correlates with an increase in RHOA levels.<sup>72</sup> The remaining 2 genes *ASPHD1* and *CDIPT1* have not been identified as high-risk genes in the development of ASD; however, both are involved in integral biological processes. Aspartate Beta-Hydroxylase Domain Containing 1 (*ASPHD1*) is an integral membrane component that has dioxygenase activity, while CDP-Diacylglycerol-Inositol 3-Phosphatidyltransferase (*CDIPT1*) catalyzes the biosynthesis of phosphatidylinositol and inositol conversion reactions.

Of the 24 genes outside of the 118 kb region designated as critical to the 16p11.2 locus, genes *MAZ*, *TAOK2*, *CORO1A* have been identified as dosage-sensitive to loss of function and *MAPK3* encodes proteins that are essential to MAP kinase signal transduction pathway. First, thousand-and-one-amino acid 2 kinase (*TAOK2*) encodes serine/threonine protein kinase that activate mitogen activated protein kinase (MAPK) pathways such as JNK, p38 and extracellular signal regulated kinases which modulates gene transcription.<sup>73</sup> In a study by Calderone de Anda *et al.*, shRNAs were employed to knockout *TAOK2* and its downstream effector genes in primary mouse cortical neurons. Investigators found that downregulation of *TAOK2* impairs basal dendrite development and alters spine formation. Noteworthy, the basal dendritic domain of neocortical PyNs receive the majority of synaptic connections.<sup>73</sup> Of significant importance is *MAPK3* which acts in the regulation of transcription, translation, and cytoskeleton rearrangement to control cell proliferation, adhesion, survival, and differentiation. In sum, it is not a single gene

rather the interaction of all the genes clustered within the 16p11.2 locus that contributes to the heterogeneous phenotypes associated with ASD.

To date, no studies have been published that evaluate the association between the genes within the 16p11.2 locus and the interneuron subtype ChC. More specifically, there has not been a study that directly examines the impact that ASD associated gene within the 16p11.2 locus may have on ChCs. Given the results from prior studies that have identified the functions of distinct genes within the 16p11.2 locus, one may speculate genes involved in brain development and function would be prime candidates. First, *MVP* is involved in nucleocytoplasmic translocation within neurons of the cerebral cortex, therefore this gene may have a global impact on the ChC developmental trajectory. The *TAOK2* gene has been identified as playing an essential role in the morphogenesis of dendrites of cortical PyN which ultimately impacts the axo-dendritic synaptic connection. However, ChCs innervate the AISs of PyNs which is an axo-axonic connection; therefore, this gene may not have an impact on ChC synaptic connections with PyNs. Last, to elucidate the impact that genes within the 16p11.2 locus have on ChCs, genetic studies utilizing single-cell RNA sequencing should be conducted to assess the genes that temporally and spatially affect ChC interneurons.

### 2.1.1 Human Phenotypes Associated with 16p.11.2 Deletion

In humans the deletion and duplication of the 16p11.2 loci is associated with a myriad of phenotypes such as dysmorphic anatomical features, abnormal behavioral patterns and altered neurological states. In particular, the 16p11.2 reciprocal CNV predispose individuals to several NDDs and other common pathological phenotypes such as abnormal head size, obesity, epilepsy, seizures, intellectual disability, schizophrenia, and ASD. Notably both the deletion and duplication present a sex bias in the development ASD and intellectual disability, whereas males harboring either CNV are most likely affected.<sup>67</sup> Most striking is that the dosage effect between the deletion and duplication of the reciprocal gene clusters produce the same pathologies with differing severities and often opposite phenotypes. The pathological severity of 16p11.2 deletion is typically more severe than the duplication, such epidemiological analyses indicate that pediatric deletion carriers have a 62.4% penetrance relative to 11.2% in duplication carriers.<sup>67</sup> While opposite phenotypes or mirror traits have been observed in the head circumference of carriers, whereas those harboring a deletion may exhibit macrocephaly and duplication carriers may have microcephaly.

Dysmorphic anatomical features that are typically associated with human carriers of 16p11.2 deletions are small cranial size, broad forehead, underdeveloped upper and lower jaws, as well as hypertelorism (increase space between eyes). Although case studies of deletion carriers have indicated populations of patient that have either microcephaly or macrocephaly, cranial size typically increase after age 2 years for individuals affected with ASD. Diffusion tensor imaging studies have indicated an increase in gray and white matter in deletion carriers, more specifically imaging has identified atypical white matter maturation in cortex of deletion carriers.<sup>67</sup> Atypical white maturation may suggest that more synaptic connectivity is present, and

it may imply that deletion carriers need to develop larger scale circuitry in order to function. In addition, 16p11.2 carrier have an increased risk for development of obesity and an overall higher body mass index than healthy and individuals harboring the duplication. *In vitro* hiPSCs of cortical neurons that harbor 16p11.2<sup>del/-</sup> showed an increase in soma size and dendrite length which suggest that in human carriers cortical size increases. Conversely, studies have indicated that 16p11.2<sup>del/-</sup> mouse models have reduced brain size and low body weight. In the 16p11.2<sup>del/-</sup> mouse models, the reduction in brain size has been linked to the decrease in the upper layer cortical projection neurons due to diminished progenitor neural pools and malformed cortical structures.<sup>67</sup>

There are several abnormal neurobehavioral profiles that are associated with 16p11.2 deletion carriers. The common neurobehavioral profiles are deficits in speech, intellectual impairment, abnormal emotional expression, as well as persistent delays and deficits in motor coordination and social skills.<sup>65</sup> Alteration in neurological states are common phenotypes in 16p11.2 deletion carriers such symptoms such as abnormal agility or clumsiness, hypotonia (decrease muscle tone) and unprovoked seizures, tremors. Abnormal behavior and altered neurological states are associated with the numerous NDDs and neuropsychiatric disorders that 16p11.2 deletion carriers develop. Unfortunately, most pathologies associated with 16p11.2 deletion present with overlapping symptoms which makes diagnosis based on behavioral patterns or neurological abnormalities challenging.

Phenotypic variability amongst carrier of 16p11.2 deletion carriers has been observed. In a study by a Shen et al., intra-familial variability in symptoms from across parent and children were observed.<sup>74</sup> Investigators identified that each family member expressed distinct phenotypes such as intellectual disability, dysmorphic facial features or ASD; these phenotypes were

associated with loss of the same length of the 16p11.2 locus.<sup>74</sup> Although, it is unclear why there is heterogeneity amongst 16p11.2 deletion carrier phenotypes, evidence suggest that additional CNVs may contribute to the variability as well as exposure to perinatal insults that may have long-term effect on offspring.<sup>65</sup>

## **2.2 Thesis Introduction**

The PFC is the region of the brain within the frontal lobe that fully develops last typically during early adulthood, in humans. PFC receives inputs from all other cortical regions and operates high-ordered cognitive processes such as decision-making, reasoning, affective and social behavior. Impairments within the PFC such as alterations in cortical circuitry are associated with cognitive and behavior deficits and PFC abnormalities have been identified in ASD patients.<sup>75</sup> Formation of synaptic connections between PyNs and GABAergic interneurons paramount to proper assembly and functioning of cortical circuitry. Moreover, at least ten GABAergic interneuron types have been identified in the cerebral cortex, they possess distinct axonal arbors that preferentially innervate subcellular compartments to control the input, integration, and output of the target cell. The ChC is an interneuron type that innervates at AIS of PyNs which allows it to control the action potential, thus it has veto-power over the neurotransmission output of the PyN.<sup>76</sup>

The impetus for conducting this project is that the Paul lab is interested in understanding how neuronal cell types and sub-types develop and achieve their final cellular identity. Apart of that the research is also aimed at understanding how their cell fate affects phenotypic expression. The chandelier cell is a major focus of the lab, although it is rare in the cortical neuronal population; it wields a profound amount of control of neurons that it innervates through its selective connection to the AIS the origin of the action potential.



### 2.3 Significance and Hypothesis

The objective of this thesis project is to test the link between 16p11.2 deletion and its impact on ChCs in the pre-frontal cortex of a mouse model; this controlled experimental system harbors neurons that are genetically labeled which allow us to unambiguously track and reproducibly assay them. To date, there has been no published studies that explore the effect of the 16p11.2 microdeletion on chandelier cells that employs a mouse model. This project is unique because it seeks to test a specific neuronal cell type in the context of an ASD mouse model and examine cellular counts and distribution within areas of the PFC. Further the results will directly associate phenotypical characteristics to ChCs found in 16p11.2<sup>del/+</sup> mouse model as compared to the wild type. Prior studies that examine biological phenotypes in humans that harbor the 16p11.2<sup>del/+</sup> corroborate that these results in the 16p11.2<sup>del/+</sup> mouse model can be biologically significant for ASD associated alterations in neuronal circuitry.<sup>65</sup>

Notably, in a study by Ariza *et al.*, postmortem human pre-frontal cortex tissue was immunostained to distinguish PV+-expressing interneurons basket cells and ChCs and the quantity of soma for each cell type was enumerated. Investigators found that the quantity and distribution of ChCs are reduced as compared to basket cells in the pre-frontal cortex tissue of ASD individuals.<sup>77</sup> However, as a limitation to this study only the basket cells were distinctly identified by presence of PV+ and vicia villosa lectin a biomarker to detect their perineuronal net; therefore, ChCs were distinguished by the lack of the latter biomarker. In a follow-up study by Amina *et al.*, postmortem human pre-frontal cortex tissue was utilized and the cartridge axonal terminals of ChCs were immunostained and enumerated. Results revealed that the density and quantity of ChCs are reduced in ASD samples as compared to control samples.<sup>78</sup> Though identification of ChCs were made by immunostaining GAT-1 positive cartridges, this method

does not discretely select for ChCs. Yet still both studies are limited by the fact that analysis of post-mortem tissue is an endpoint which cannot confidently confirm that ChC reduction is due to ASD or other pathological insults incurred prior to death.

Since each pyramidal cell obtains inputs from one or more ChCs, a single ChC is capable of innervating hundreds of pyramidal cells, thereby coordinating their activity. ChCs have a direct impact on cortical circuitry output and a reduction in ChCs can potentially globally effect circuitry and ultimately generate an imbalance in the excitation/inhibition ratio. The relationship between inhibition or increase in the rate of PyN cell firing in the cortex has produced conflicting outcomes from both mouse models and human ASD patients.

Work published by Antoine *et al.*, examined how ASD phenotypes caused by specific genes evaluated in 4 distinct mouse models ( $Fmr1^{-/y}$ ,  $Cntnap2^{-/-}$ ,  $16p11.2^{del/+}$ ,  $Tsc2^{+/-}$ ) produce a similar increase in E/I conductance ratio in the somatosensory region of the PFC.<sup>46</sup> Data from this study provides compelling evidence that circuitry signal output is affected by specific genotypes.<sup>46</sup> In a study by Bertero *et al.*, resting state fMRI on human pediatric cohorts diagnosed with either typical development or a NDDs.<sup>79</sup> The investigators demonstrated that carriers of the heterozygous deletion  $16p11.2^{del/+}$  have diminished pre-frontal connectivity and disrupted long-range functional coupling within temporal parietal regions. Furthermore, investigators conducted fMRI on mice and found that diminished pre-frontal connectivity, disrupted thalamo-prefrontal connections as well as reduced long-range low frequency neural synchronization occurs in mice with the  $16p11.2^{del/+}$  deficiency.<sup>79</sup> Taken together, the prior evidence suggests that the microdeletion of  $16p11.2$  and a reduction in the number of ChCs may be contributing risk factors in the development of ASD.

We hypothesized that mice harboring a deletion that is a syntenic region to the human 16p11.2 microdeletion would have altered ChC counts and distribution in the pre-frontal cortex as compared to the WT mouse. The aim of this thesis was to determine if there is an alteration in density and distribution of ChCs boutons that contact pyramidal neurons in the PFC.

## 2.4 Materials and Methods

**Table 2.4.1 List of Materials Used**

<b>Materials</b>		
<b>Material</b>	<b>Source</b>	<b>Identifier</b>
<b>Animal Models</b>		
Mouse: 16p11.2 <sup>del/+</sup>	Jackson Laboratory	<i>JAX stock# 013128</i>
Mouse: Unc5b-2A-CreER; Nkx2.1-Flp; Ai65	Cold Spring Harbor Laboratory	Dudok et. al. 2021, Neuron
<b>Antibodies and Blocking serum</b>		
Mouse anti-Ankyrin G	EMD Millipore NeuroMab	MABN466MI
Rabbit anti-GAT-1	Chemicon/Millipore	AB1570
Donkey anti-mouse-647 nm	ThermoFisher Scientific	A32766
Donkey anti-Rabbit-488 nm	ThermoFisher Scientific	A32790
Neuro Trace 435/455 nm	Invitrogen	N21479
<b>Software and Algorithm</b>		
CellProfiler™ v4.2.1	Broad Institute	<a href="https://cellprofiler.org/">https://cellprofiler.org/</a>
JASP v0.16.3	JASP Team (2022)	<a href="https://jasp-stats.org">https://jasp-stats.org</a>
Zen 3.2 (Blue edition) 2020	Carl Zeiss Microscopy GmbH	<a href="https://www.zeiss.com/microscopy/us/products/microscope-software.html">https://www.zeiss.com/microscopy/us/products/microscope-software.html</a>

All experiments were carried out in accordance with the guidelines of the Institutional Animal Care and Use Committee (IACUC) of Penn State University and following protocol 00781. Sample conditions included male and female mice from both wild-type and (16p11.2<sup>del/+</sup>) litters sacrificed at post-natal intervals (17, 28, and 31) days, subsequently brains were perfused transcardially with PBS and 4% paraformaldehyde in 0.1M PBS and finally extracted

from the skull. All mice were provided with access to food and water *ad libitum* and maintained at 12-hour light-dark-cycle.

To test the hypothesis, genetically engineered mice harboring the 16p11.2<sup>del/+</sup> were bred to mice harboring the *Unc5b-Cre; Nkx2.1-Flp; Ai65* driver reporter line. The *Unc-5b* signifies the Unc-5 Netrin receptor B gene that encodes members of netrin family of receptor proteins that binds to the netrin1 ligand; it has many functions, notably it is required for negative regulation in axon guidance. UNC5b is highly specific to ChCs and it has been postulated that it netrin1-UNC5b binding may facilitate cell-cell recognition.<sup>80</sup> Nkx2.1 is a transcription factor expressed in the medial ganglionic eminence of the developing embryo, a neurogenic zone that contributes to the major fraction of interneurons in mice. Ai65 is a tdTomato reporter that is responsive to the combined expression of Cre and Flp recombinase in a cell.

Mice brain tissue were coronally sectioned at 30 µm thickness with a vibratome (Leica VT1000S). Multiple sections per mouse were sliced surrounding the reference point determined in the Mouse atlas as designated by bregma point. To survey the neuronal cell bodies and the axo-axonic connections between ChC boutons and the AIS of pyramidal cells, numerous sections of each brain were selected for immunofluorescent staining. Fluorescently conjugated antibodies against the following proteins were utilized: GABA transporter 1 (GAT-1) functions in pre-synaptic axon re-uptake of neurotransmitters, ankyrin-G (AnkG) a scaffolding protein that acts in the AIS, and Fluorescent Nissl (Neuro Trace™) stains ribosomal RNA associated with the rough endoplasmic reticulum of brain cells.

Immunohistochemical staining of each section was performed utilizing the following optimized general protocol. Each microwell contained 5-10 tissue sections to ensure that each section achieved optimal absorption of reagents. First, the tissue sections were permeabilized

and then blocked. The blocking step was performed to reduce background signal caused by the primary and secondary antibodies binding to non-specific sites. Blocking and permeabilization cocktail of normal donkey serum, 10% Triton X-100, and 1X PBS was added in a total of 350  $\mu$ L per well and then the plate was shaken at room temperature for 2 hours. After the 1X PBS wash, the primary antibody cocktail consisting of dilution of each mouse serum anti- AnkG, rabbit anti-GAT-1 in 10% Triton X-100, and 1X PBS was added at 350  $\mu$ L per well and shaken at 4°C for 72 hours.

Following the 1X PBS wash step, the secondary antibody cocktail containing donkey anti-mouse-conjugated to the fluorophore 647 nM and donkey anti-rabbit-conjugated to the fluorophore 488 nM diluted in (1:500) of reagents 10% Triton X-100, and 1X PBS for a total of 350  $\mu$ L per well. The plate was shaken at room temperature for 2 hours. Subsequently, a cocktail containing Neuro Trace™-435 nM in a (1:300) dilution of 1X PBS was added at 350  $\mu$ L per well, then the plate was shaken at room temperature for 20 minutes. Finally, a 1X PBS wash was performed prior to mounting each immunostained section onto a glass slide.

Images have been visualized through high resolution confocal microscopy (LSM 900, Zeiss) at 20X magnification. The magnification power was selected based on the ability to visual the most AIS per the field of view for a section. The following cortical regions which are predominantly associated with ASD deficits have been selected for testing: cingulate cortex area 1 and 2 (Cg1 and Cg2), the prelimbic cortex (PrL) primary and secondary motor cortex (M1 and M2) in addition, multiple areas within the primary somatosensory cortex (S1) and secondary somatosensory cortex (S2). Additional regions within the cortex were also sectioned for evaluation. On every image the region of interest (ROI) was selected by manually demarcating each region with rectangles by the Zen Blue edition software tools, ROI were selected based on

the mouse brain atlas map at corresponding bregma points. Refer to Appendix A for images of the coronal mouse maps used. More than 1,600 images were acquired in total from all 6 brains and across 9-10 areas of the PFC. However, after an intermediate quality control step which trimmed and selected images that had the best visual integrity of each region, only 8 areas were selected. A final total of more than 1,200 images were acquired across all brains, refer to Appendix A for details.

To determine the number and distribution of ChC boutons and ChC bouton contacts onto the AISs of the postsynaptic neurons, an image analysis program CellProfiler™ has been employed to count the number of ChC boutons and AISs. CellProfiler™ is an open-source software tool that extracts information from biological images and allows the end-user to quantify the data obtained from biological images.<sup>81</sup> Enumeration of ChCs were based on the following parameters. The ChCs are genetically labeled with a conditional RFP reporter and postsynaptic AIS were labeled with AnkG. The boutons of the ChC cartridges were stained for GAT-1 pre-synaptic protein to distinguish between a contact and an active synapse innervation. The customized CellProfiler analytic pipeline “*AB-CHC-bouton-counts-8.cpproj*” was generated to quantify the AISs and boutons as well as discern active GAT-1 bouton innervation on the AIS as described as a supplement in Appendix B.

The statistical analysis was performed using JASP software an open-source program.<sup>82</sup> A total of 6 brains were processed and were comprised of the following: (WT male n =2; 16p11.2<sup>del/+</sup> male n = 3; and 16p11.2<sup>del/+</sup> female n = 1). Notably, the total number of brain areas imaged were variable across each brain collected whereas some brains had zero images in a region while others had numerous. All brain image was collected and stratified based on region into a distinct folder, a total of 8 distinct folders of images representing 8 PFC areas were analyzed. The

parameters assessed were the following: the number of bouton contacts on the AIS, number of bouton contacts on AIS that contain GAT-1 (deemed active contact), area shape of the AIS, and area shape of AIS major axis length. The mean of each parameter was calculated and used in either the ANOVA or ANCOVA statistical design within the JASP software.

## **2.5 Results**

### **2.5.1 Design of Data Analysis**

To address the hypothesis that the ChC bouton cartridge number will be altered in the 16p11.2<sup>del/+</sup> model as compared to the wild-type, the relationship between ChC bouton contact to the AIS of the pyramidal cell (ChC/AIS-PyN) was investigated. The images acquired from the following areas were used in all analyses: Cg1, M1, M2, PrL, RegFS (frontal cortex, area 3, primary sensory cortex, jaw region), RSD (retrosplenial dysgranular cortex), RSGc (retrosplenial granular cortex c, region), and S1 (primary somatosensory cortex areas: dysgranular zone, forelimb region, jaw region, upper lip) as well as small parts of the secondary somatosensory cortex. Since only a single female 16p11.2<sup>del/+</sup> brain was processed, data acquired from the female were filtered out of all analyses, leaving only data from male brains WT and 16p11.2<sup>del/+</sup> to be analyzed.

### **2.5.2 Cell Number and Distribution**

First, the number of ChC bouton contacts on the AISs of PyNs were quantified by evaluating these parameters: the number of ChC boutons contacts versus the area of the AIS of PyNs within each PFC area. Data was analyzed using ANCOVA to account for effects from covariates such as the variability in the AIS major axis length across different AISs in each brain region. Most astonishing, the results illustrated that ChC bouton contact numbers on the AIS are

relatively similar in both WT and 16p11.2<sup>del/+</sup> across all areas of the PFC surveyed, with exception for the PrL and to a lesser extent S1. Three post hoc analyses were performed to determine if the mean difference in the ChC boutons/AIS-PyNs between genotypes for each region is significant. As displayed in table 2.5.2 a., the number of ChC bouton innervations were significantly lower in the 16p11.2<sup>del/+</sup> model within both the PrL ( $p < 0.001$ , Cohen's  $d = 0.792$ ) and S1 ( $p < 0.001$ , Cohen's  $d = 0.559$ ) as compared to the WT. Refer to figures 2.5.2 a-i which illustrates a summary of WT vs. 16p11.2<sup>del/+</sup> number of ChC boutons/AIS-PyNs across 8 regions of the PFC or a comparison of the number of ChC boutons/AIS-PyNs between genotypes in a singular area, respectively.

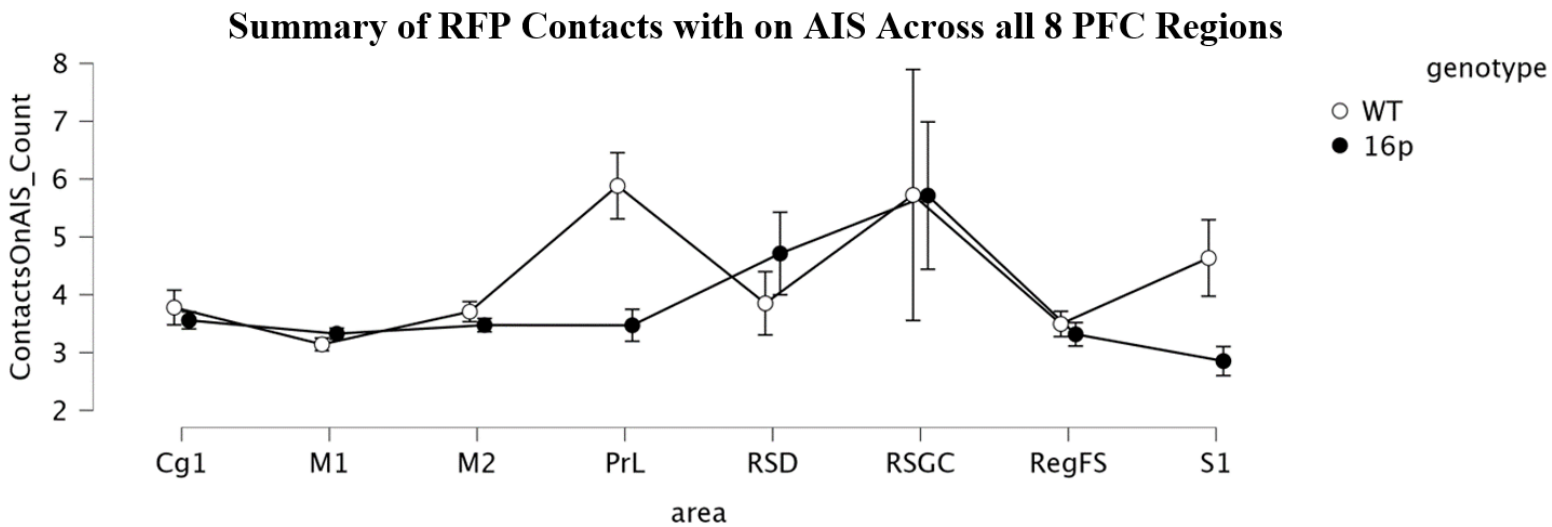
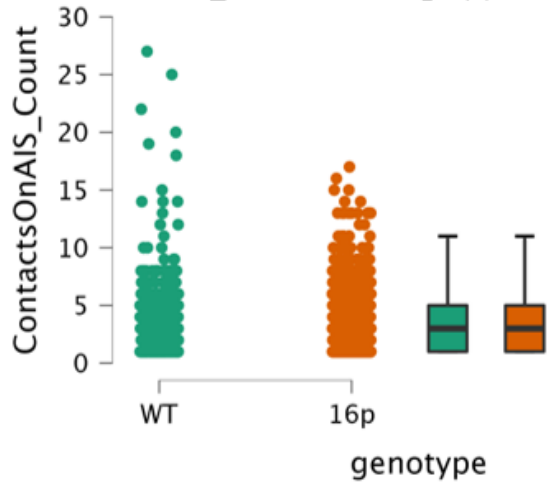


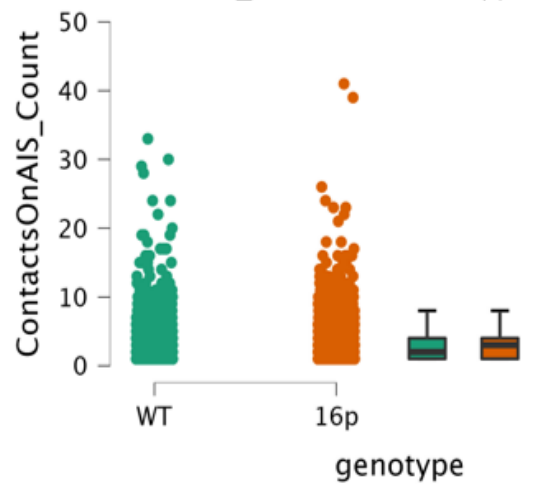
**Figure 2.5.2 (a):** Graphical representation of the ANCOVA analysis of all ChC bouton contacts on AISs area across all 8 regions



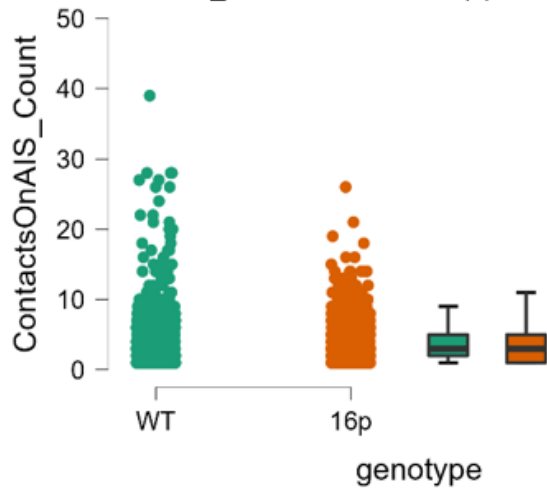
**ContactsOnAIS\_Count: area: Cg1 (b)**



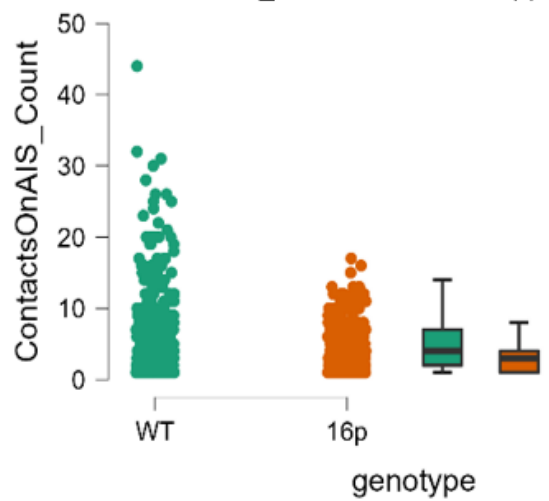
**ContactsOnAIS\_Count: area: M1 (c)**



**ContactsOnAIS\_Count: area: M2 (d)**

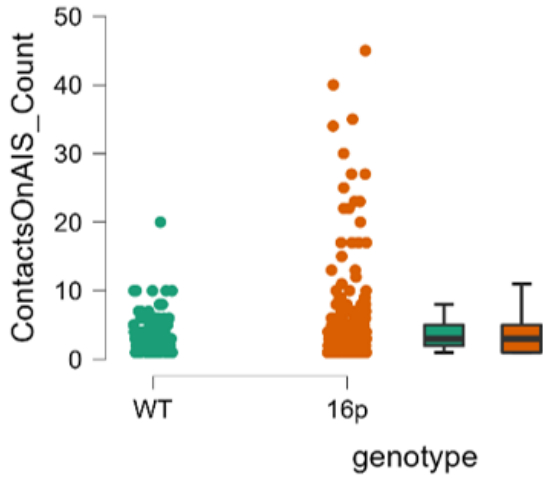


**ContactsOnAIS\_Count: area: PrL (e)**

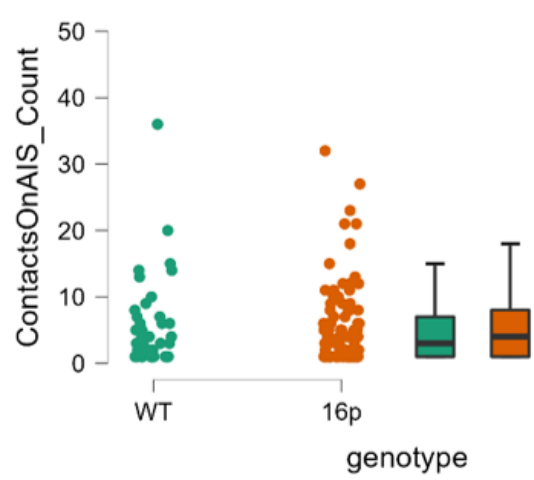


**Figures 2.5.2 (b-e):** Graphical representation of the ANCOVA analysis of all ChC bouton contacts on AISs area across 4 regions Cg1, M1, M2 and PrL

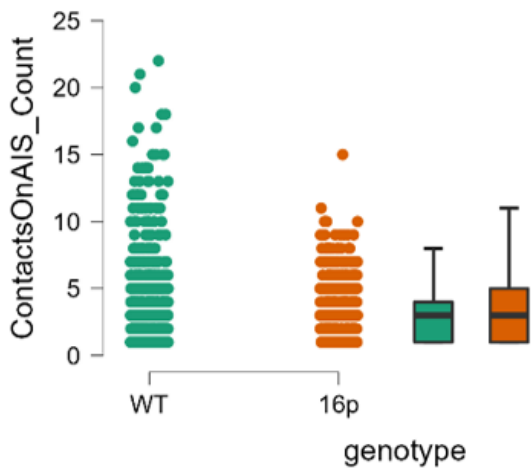
**ContactsOnAIS\_Count: area: RSD (f)**



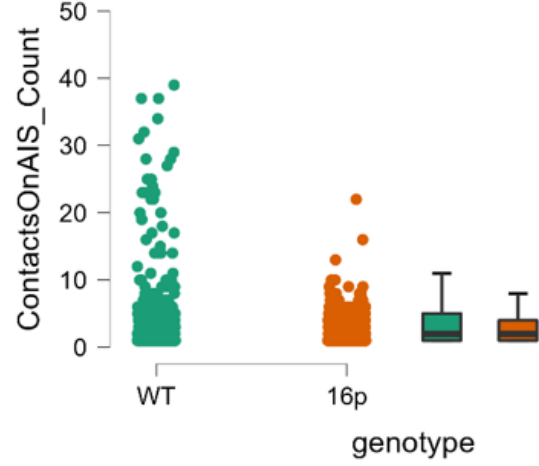
**ContactsOnAIS\_Count: area: RSGC (g)**



**ContactsOnAIS\_Count: area: RegFS (h)**



**ContactsOnAIS\_Count: area: S1 (i)**



**Figures 2.5.2 (f-i):** Graphical representation of the ANCOVA analysis of all ChC bouton contacts on AISs area across 4 regions RSD, RSGc, RegFS and S1

**Table 2.5.2 (a): Summary of RFP Contacts on AIS Across all 8 PFC Regions**

ANCOVA Post Hoc Comparisons - genotype \* area

		Mean Difference	SE	t	Cohen's d	<u>P</u> tukey	<u>P</u> bonf
WT Cg1	16p Cg1	0.362	0.177	2.043	0.112	0.801	1.000
WT M1	16p M1	-0.028	0.087	-0.317	-0.009	1.000	1.000
WT M2	16p M2	0.416	0.111	3.743	0.129	0.017 *	0.022 *
WT PrL	16p PrL	2.556	0.221	11.560	0.792	< .001 ***	< .001 ***
WT RSD	16p RSD	-0.878	0.373	-2.353	-0.272	0.583	1.000
WT RSGC	16p RSGC	0.072	0.612	0.118	0.022	1.000	1.000
WT RegFS	16p RegFS	0.363	0.185	1.966	0.113	0.844	1.000
WT S1	16p S1	1.802	0.240	7.493	0.559	< .001 ***	< .001 ***

*Note.* P-value adjusted for comparing a family of 16

\* p &lt; .05, \*\* p &lt; .01, \*\*\* p &lt; .001

Although the number of ChC bouton contacts on AIS PyNs can be enumerated by simply the RFP genetic label of the ChC cartridge itself, the presence of synaptic GABA transporter GAT-1 within the ChC presynaptic bouton confirms that it's a functional innervation. The analysis of ChCs boutons with GAT-1 contacts on AISs of PyNs is comparable to the prior analysis of ChC bouton contacts alone, refer to figures 2.5.2 j-r and table 2.5.2 b. Overall, there is no significant difference in ChC bouton innervation of AISs of PyNs across most of the PFC areas in WT versus 16p11.2<sup>del/+</sup>, except for PrL and S1. These results corroborate that there is a decrease in ChC contact number in 16p11.2<sup>del/+</sup> model as compared to WT specifically in PrL and S1.

### Summary of RFP Contacts with GAT-1 on AIS Across all 8 PFC Regions

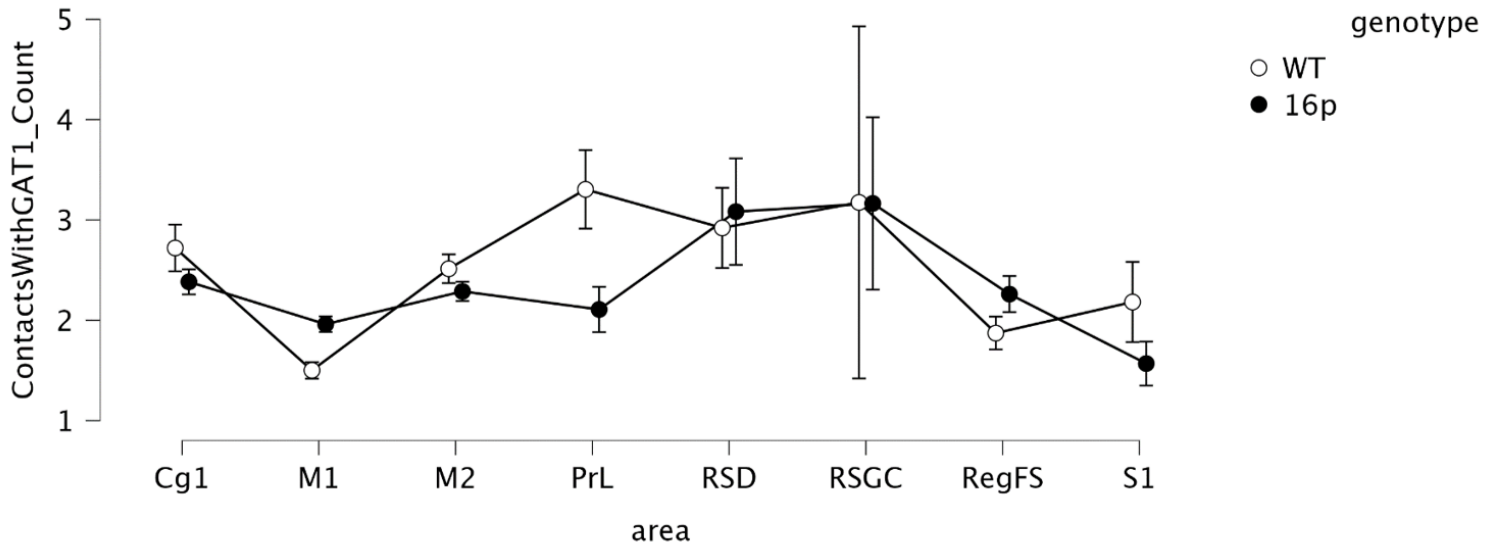
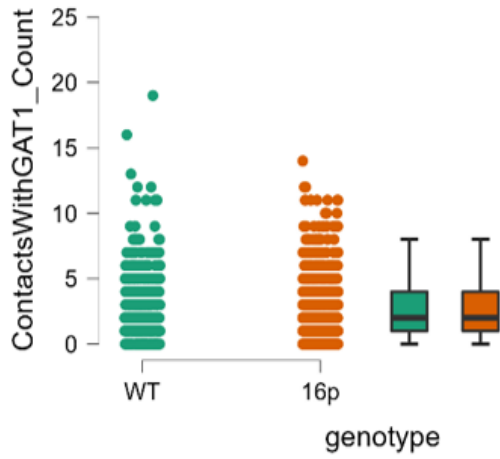
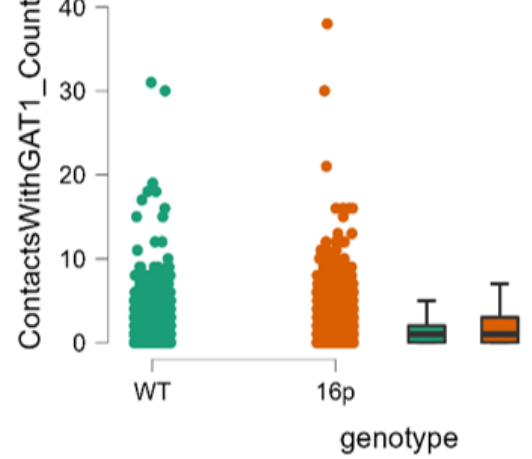


**Figure 2.5.2 (j):** Graphical representation of the ANCOVA analysis of all ChC boutons with GAT-1 contacts on AISs across all 8 regions

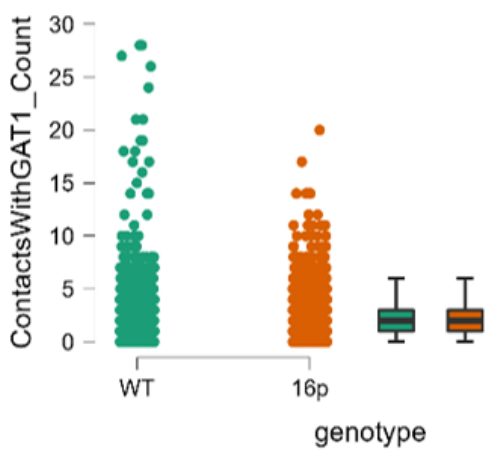
**ContactsWithGAT1\_Count: area: Cg1 (k)**



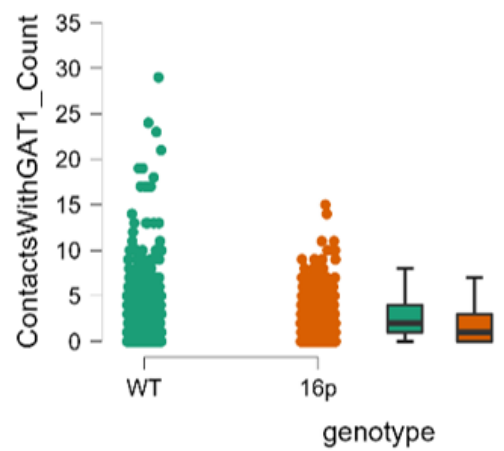
**ContactsWithGAT1\_Count: area: M1 (l)**



**ContactsWithGAT1\_Count: area: M2 (m)**

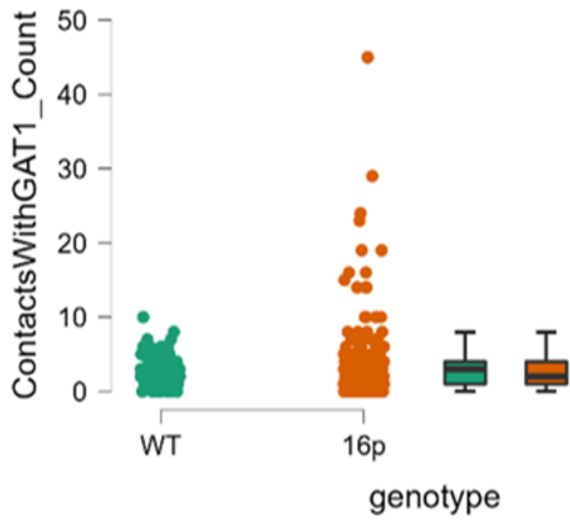


**ContactsWithGAT1\_Count: area: PrL (n)**

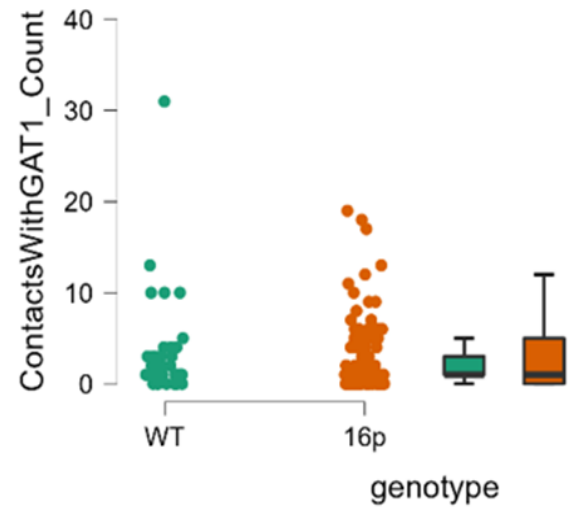


**Figures 2.5.2 (k-n):** Graphical representation of the ANCOVA analysis of all ChC boutons with GAT-1 contacts on AISs area across 4 regions Cg1, M1, M2 and PrL

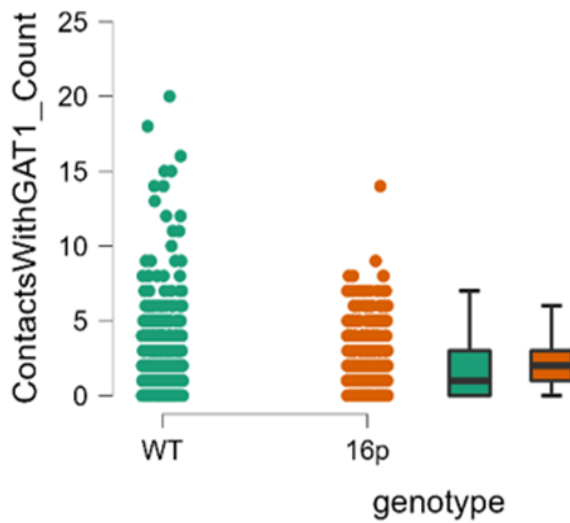
**ContactsWithGAT1\_Count: area: RSD (o)**



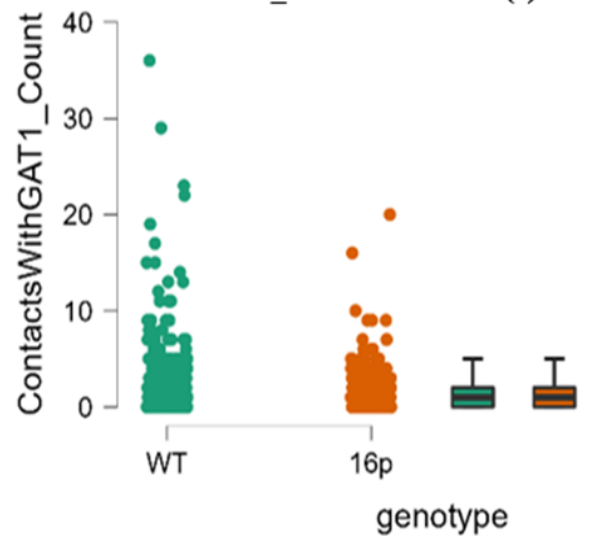
**ContactsWithGAT1\_Count: area: RSGC (p)**



**ContactsWithGAT1\_Count: area: RegFS (q)**



**ContactsWithGAT1\_Count: area: S1 (r)**



**Figures 2.5.2 (o-r):** Graphical representation of the ANCOVA analysis of all ChC bouton contacts on AISs area across 4 regions RSD, RSGc, RegFS and S1

**Table 2.5.2 (b): Summary of RFP Contacts with GAT-1 on AIS Across all 8 PFC Regions**  
**Post Hoc Comparisons - genotype \* area**

		Mean Difference	SE	t	Cohen's d	P <sub>tuke</sub>	P <sub>bout</sub>
WT Cg1	16p Cg1	-9.120	5.859	-1.557	-0.052	0.957	1.000
WT M1	16p M1	-21.373	3.588	-5.957	-0.122	< .001 ***	< .001 ***
WT M2	16p M2	-14.831	3.823	-3.879	-0.085	0.008 **	0.010 **
WT PrL	16p PrL	-7.343	7.231	-1.015	-0.042	0.999	1.000
WT RSD	16p RSD	11.605	11.473	1.012	0.066	0.999	1.000
WT RegFS	16p RegFS	-81.471	6.772	-12.030	-0.464	< .001 ***	< .001 ***
16p RegFS	WT S1	88.074	7.949	11.080	0.502	< .001 ***	< .001 ***
WT S1	16p S1	-23.521	9.518	-2.471	-0.134	0.428	1.000

**Note.** P-value adjusted for comparing a family of 14

\* p < .05, \*\* p < .01, \*\*\* p < .001

### 2.5.3 Chandelier Cell Bouton Size and Number of AIS Contact

Synaptic size is directly related to its strength such that changes in strength is reflected in an alteration in the size of the synapses, with all synaptic components--active zone, postsynaptic density, and bouton--becoming larger with increasing strength.<sup>83,84</sup> Such changes in synapse size could play a significant role in mediating optimal cognitive function and experience-dependent plasticity alongside synapse formation, elimination, and stabilization.<sup>85-88</sup> Hence, we evaluated the ChC bouton size alterations in 16p11.2 del/+ against wild-type animals across brain areas.

The size of ChC boutons as determined by RFP+ area on the AIS was analyzed, and most regions had no significant difference between genotypes. Contrary to the last analysis the ChC bouton area did not differ in genotype for the PrL and S1, meaning that while the number of AIS synapses were lower in 6p11.2<sup>del/+</sup> model the synaptic strength did not change. Instead, the RegFS which is the frontal area of the primary somatosensory cortex, showed a significant

increase in ChC bouton size on the AIS ( $p < 0.001$ , Cohen's  $d = 0.464$ ) in the  $16p11.2^{del/+}$  model as compared to the WT. Refer to figures 2.5.3 a-b. and table 2.5.3 a.

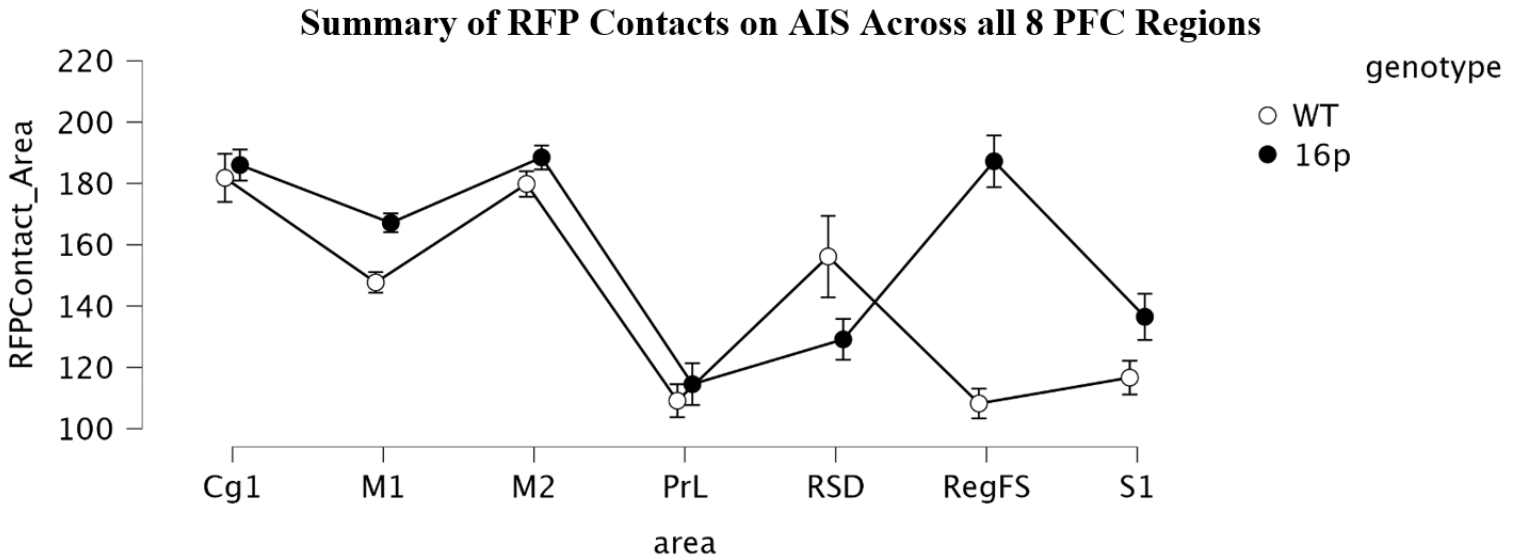


**Figure 2.5.3 (a):** Graphical representation of the ANOVA analysis of all ChC bouton contacts on AISs across all 8 regions

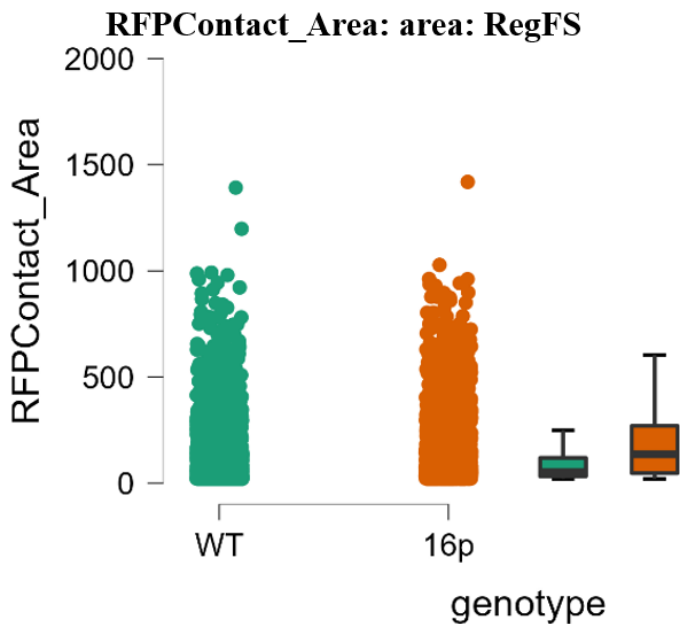


**Figure 2.5.3 (b)** Comparing the number of ChC bouton contacts on AISs of PyN between WT and  $16p11.2$  deletion within RegFS



Post hoc analyses were performed to determine if the mean difference in the ChC bouton size between genotypes for each region is significant. As displayed in table 2.5.3 a., RegFS generated  $p < 0.001$ , which indicates that the difference between mean ChC boutons size of WT and 16p11.2<sup>del/+</sup> is significant.

**Table 2.5.3 (a): Summary of RFP Contacts on AIS Across all 8 PFC Regions**

**ANOVA Post Hoc Comparisons - genotype \* area**

		Mean Difference	SE	t	Cohen's d	<u>P<sub>tukey</sub></u>	<u>P<sub>bonf</sub></u>
WT Cg1	16p Cg1	-9.120	5.859	-1.557	-0.052	0.957	1.000
WT M1	16p M1	-21.373	3.588	-5.957	-0.122	< .001 ***	< .001 ***
WT M2	16p M2	-14.831	3.823	-3.879	-0.085	0.008 **	0.010 **
WT PrL	16p PrL	-7.343	7.231	-1.015	-0.042	0.999	1.000
WT RSD	16p RSD	11.605	11.473	1.012	0.066	0.999	1.000
WT RegFS	16p RegFS	-81.471	6.772	-12.030	-0.464	< .001 ***	< .001 ***
WT S1	16p S1	-23.521	9.518	-2.471	-0.134	0.428	1.000

**Note.** P-value adjusted for comparing a family of 14

\*  $p < .05$ , \*\*  $p < .01$ , \*\*\*  $p < .001$

In particular, ASD phenotypes exhibit atypical response to sensory stimuli in both human and mouse models, whereas in mice locomotion and startle response are abnormal.<sup>67</sup> Electrophysiological studies employing this specific 16p11.2<sup>del/+</sup> mouse model have demonstrated that this microdeletion is associated with increased excitation–inhibition (E/I) ratio in somatosensory cortex.<sup>46</sup> The fact that the difference between the ChC bouton sizes on AISs in WT and 16p11.2<sup>del/+</sup> were similar within most PFC areas suggests that the results are not specious and perhaps such differences between WT and 16p11.2<sup>del/+</sup> in specific areas reflects a biological difference in E/I ratio in circuits associated with ASD.

To verify that the ChC boutons size identified as contacting the AISs is functional, evaluation of ChC boutons that express GAT-1 were assessed. The results from this subsequent analysis were concordant with the prior analysis, where the GAT1+ ChC bouton size were increased in 16p11.2<sup>del/+</sup> compared to the WT in RegFS. Refer to figures 2.5.3 c-d and table 2.5.3 b.

### Summary of RFP Contacts with GAT-1 on AIS Across all 8 PFC Regions

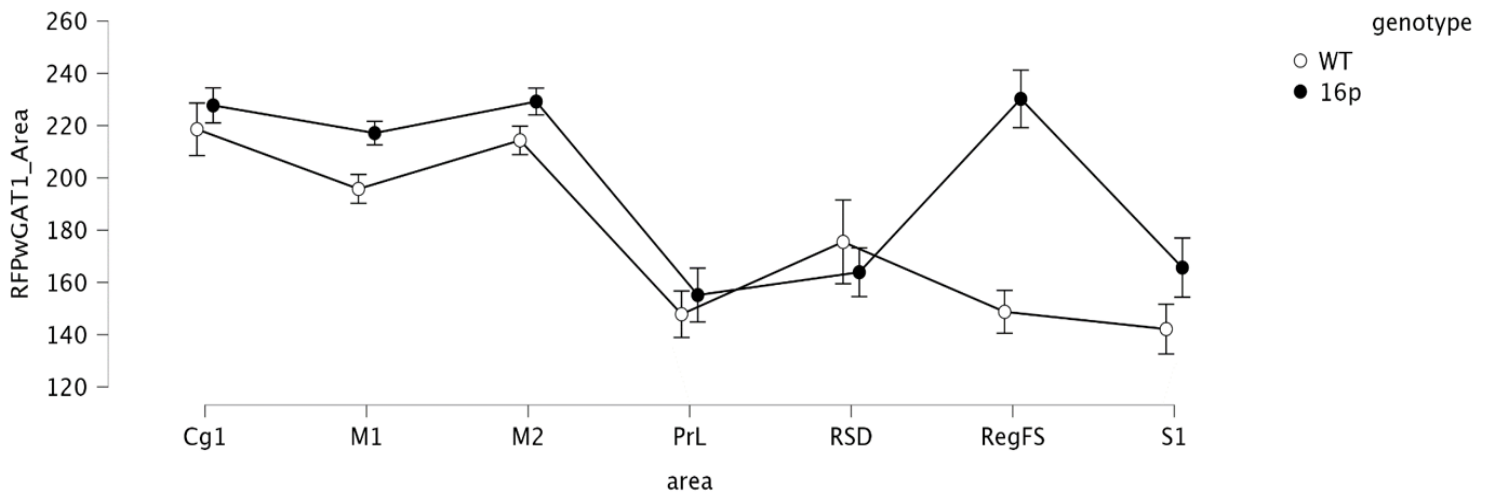


**Figure 2.5.3 (c):** Graphical representation of the ANOVA analysis of all ChC bouton contacts with GAT-1 on AISs across all 8 regions

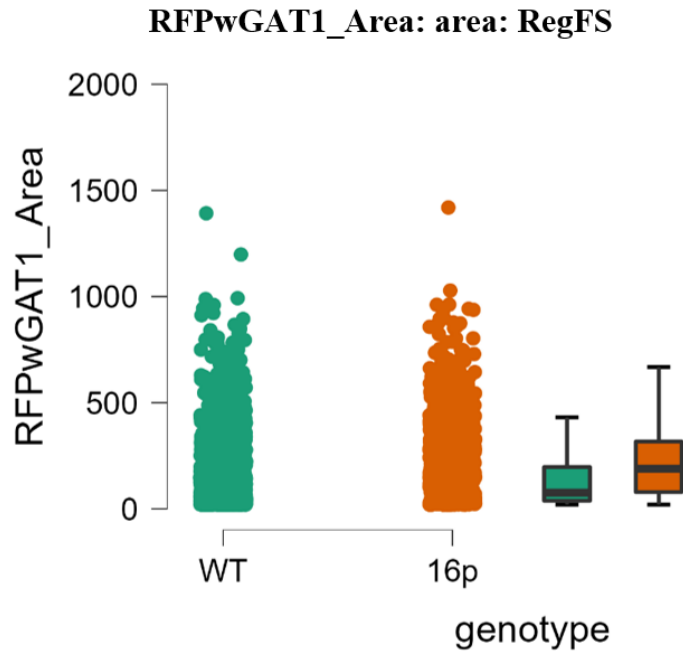


**Figure 2.5.3 (d)** Comparing the number of ChC bouton contacts with GAT-1 on AISs of PyNs between WT and 16p11.2 deletion within RegFS

**Table 2.5.3 (b): Summary of RFP Contacts with GAT-1 on AIS Across all 8 PFC Regions**

**ANOVA Post Hoc Comparisons - genotype \* area**

		Mean Difference	SE	t	Cohen's d	<u>P</u> tukey	<u>P</u> bonf
WT Cg1	16p Cg1	-9.120	5.859	-1.557	-0.052	0.957	1.000
WT M1	16p M1	-21.373	3.588	-5.957	-0.122	< .001 ***	< .001 ***
WT M2	16p M2	-14.831	3.823	-3.879	-0.085	0.008 **	0.010 **
WT PrL	16p PrL	-7.343	7.231	-1.015	-0.042	0.999	1.000
WT RSD	16p RSD	11.605	11.473	1.012	0.066	0.999	1.000
WT RegFS	16p RegFS	-81.471	6.772	-12.030	-0.464	< .001 ***	< .001 ***
WT S1	16p S1	-23.521	9.518	-2.471	-0.134	0.428	1.000

**Note.** P-value adjusted for comparing a family of 14

\* p < .05, \*\* p < .01, \*\*\* p < .001

## CHAPTER 3: CONCLUSIONS

### 3.1 Discussion

The elusive chandelier cell with its rare population number, has highly intricate arbors that are arranged into vertical array cartridges that terminate with boutons, which innervate the sub-cellular AIS of PyNs, and thus exert vetoing power over PyN. There has been a burgeoning interest in ChCs since several studies relating neurological disorders such as schizophrenia, epilepsy and ASD have shown alterations in the ChC sub-type.<sup>50,89</sup> This study examined the relationship between the number of ChC bouton contacts on AIS of PyNs in wild-type and the 16p11.2<sup>del/+</sup> mouse model. In the study we evaluated mice brain tissues at post-natal days (17,28 and 31). It has been demonstrated that ChC between P18 and P90 exhibit stable morphology and distribution, though at P17 ChC are still not completely mature their shape and final position within the laminar layer should be consistent with P18.<sup>49</sup>

Results from the study indicate that both the prelimbic and somatosensory cortex differed in ChC bouton innervation of AISs of PyN between wild-type and 16p11.2<sup>del/+</sup>. Notably, both the PrL and S1 have reduced numbers of ChC bouton innervations in the 16p11.2<sup>del/+</sup> without affecting their bouton sizes. This could be due to decrease in number of boutons per ChC or an overall decrease in ChC cell numbers. In this study we did not measure area specific changes in ChC cell bodies. The PrL and the infralimbic cortices are a part of the medial PFC that are involved in relaying signals to and from the amygdala and hippocampus area. Moreover, these area function differentially to manage context-dependent behavior which are motivated by processing the stimuli from the environment. Both areas play a role in adapting to changes in environmental cues. In particular the PrL has been implicated in adaptation to fear and drug-

seeking patterns.<sup>90</sup> Most important malfunction in synaptic circuitry within PrL have been associated with atypical social behavior.

Abnormalities in the PrL area have been found in ASD patients; this supports the fact that ASD phenotypes such as atypical social engagements may be partially due to alterations within the PrL. In an *in vivo* mouse study by Lu *et al.*, investigators showed that a subset of ChCs which occupy layer 2 within the PrL and selectively receive inputs from PyNs that project to contralateral cortex.<sup>91</sup> Moreover, another subset of ChCs preferentially innervate bilateral PyNs within the PrL, thus suggesting that ChC exhibit highly directional and selectivity in their connectivity.<sup>91</sup> Therefore, alterations in ChC bouton contact numbers within areas of PrL could potentially have differential local impact within PrL microcircuitry, but also affect the global integration and output from the PrL.

Another finding of the study was that within the somatosensory region there is difference between ChC bouton contacts on the AISs of PyNs in WT and 16p11.2<sup>del/+</sup>. It is well established that 90% of ASD individuals exhibit atypical (hypo or hyper) response to sensory stimuli such as (auditory, gustatory, olfaction, tactile, visual).<sup>92</sup> Studies of the mouse somatosensory cortex have demonstrated that individual ChCs contact 30-50% of PyNs most proximal to their axonal arbor and there is high variability in the distribution and density of these innervations.<sup>49</sup>

First, within the RegFS (frontal area of somatosensory cortex) of 16p11.2<sup>del/+</sup> the ChC bouton sizes on AISs of PyNs were strikingly higher as compared to the WT. The data suggests that ChCs may preferentially exert stronger inhibitory control within RegFS of the 16p11.2<sup>del/+</sup> model. Since this preliminary study only identifies the presence and quality of contacts the functional role for this increase can only be speculated. Studies that thoroughly compare

arborization patterns and further test circuit output via electrophysiological testing would provide more insight. Second, the region designated as the primary somatosensory (S1) in this study which encompasses all somatosensory areas and parts of the secondary somatosensory region also differs in the number of ChC boutons that contact the AIS of PyNs across WT and 16p11.2<sup>del/+</sup>. Unlike the RegFS, the number of 16p11.2<sup>del/+</sup> ChC boutons contacts are less than the WT on the AIS of PyNs. A reduction in the number of ChC bouton contacts in 16p11.2<sup>del/+</sup> as compared to WT suggests that excitatory signal output may be higher in this region due to reduced quantity of inhibitory ChCs. Though prior studies have shown in mice aged P16-25 synaptic transmission of ChCs in layers 1 and 2 depend on the resting membrane potential of the PyN,<sup>49</sup> Further functional testing to determine if the decrease in ChC bouton contact number correlates with an increase in excitatory transmission of PyNs will be necessary to clarify this relationship.

### **3.2 Summary of Significant Findings**

To date there has not been any publications of studies specifically evaluating the number of ChCs innervation on AISs of PyNs in the context of 16p11.2<sup>del/+</sup> mouse model of ASD. Yet more novel is that this study employs unambiguous identification of the ChC itself, via a specific genetic label, thus ensuring that ChC are distinguished from other PV+ interneurons such as basket cells. The outcome from this preliminary study generated several significant findings.

First, surveying the number of ChC boutons contacts on AIS in PyNs in WT versus 16p11.2<sup>del/+</sup> across 8 distinct regions of the PFC demonstrate that there is no significant difference in ChC cell innervation across most of the regions. However, there were regions such as the PrL, RegFS and S1 that had a significant difference in ChC bouton innervation between

WT and 16p11.2<sup>del/+</sup>. Second, the number of ChC bouton contacts on AISs of PyNs within the PrL differ between WT and 16p11.2<sup>del/+</sup>, where the quantity of ChC bouton contacts decreased within the 16p11.2<sup>del/+</sup> model. Finally, the number of ChC bouton innervations on AISs of PyNs within the region designated as S1 in this study and the RegFS differ between WT and 16p11.2<sup>del/+</sup>. In S1 region, the number of ChC contacts were fewer in the 16p11.2<sup>del/+</sup> model. While in RegFS, ChC bouton size were considerably more in the 16p11.2<sup>del/+</sup> model.

### **3.3 Future Directions**

In sum, this preliminary study has revealed that there is indeed a significant area dependent association between 16p11.2<sup>del/+</sup> and alterations in the number of ChC bouton contacts on the AIS of PyNs. Additional studies will need to be performed to fully elucidate how the loss of the genomic cluster within 16p11.2 affects PyNs AIS innervation by ChCs. Due to time constraints, this study has only assessed changes in the male mice of 16p11.2<sup>del/+</sup> model. Subsequent studies will collect a larger sample size of sexes and age matched mice from neonate P7 to P180 adult. Primarily, experiments to clarify the role that 16p11.2<sup>del/+</sup> has on ChC morphology, connectivity, and the overall developmental trajectory will be conducted. These initial experiments will investigate neurite branching patterns, arbor lengths and layer localization between 16p11.2<sup>del/+</sup> and WT.

In rodents, The amygdala and other brain structures send inputs to the PrL cortex to integrate in order to gate fear expression through signal projections back to the amygdala.<sup>91</sup> In addition, in rodents it has been indicated that PrL modulates or integrates signals which provide proper adaption to changes in their experimental environment. In the study there was significant loss in the number of ChC bouton innervations within PrL of 16p11.2<sup>del/+</sup>, in fact substantially fewer ChC boutons contacts were made in the experimental model. To determine if ChC bouton

numbers have a biological impact on the PrL circuit, a subsequent study to restore the number of ChCs that innervate AISs of PyNs will be performed.



## Appendix A      Tables of ROI and Mouse Atlas Images

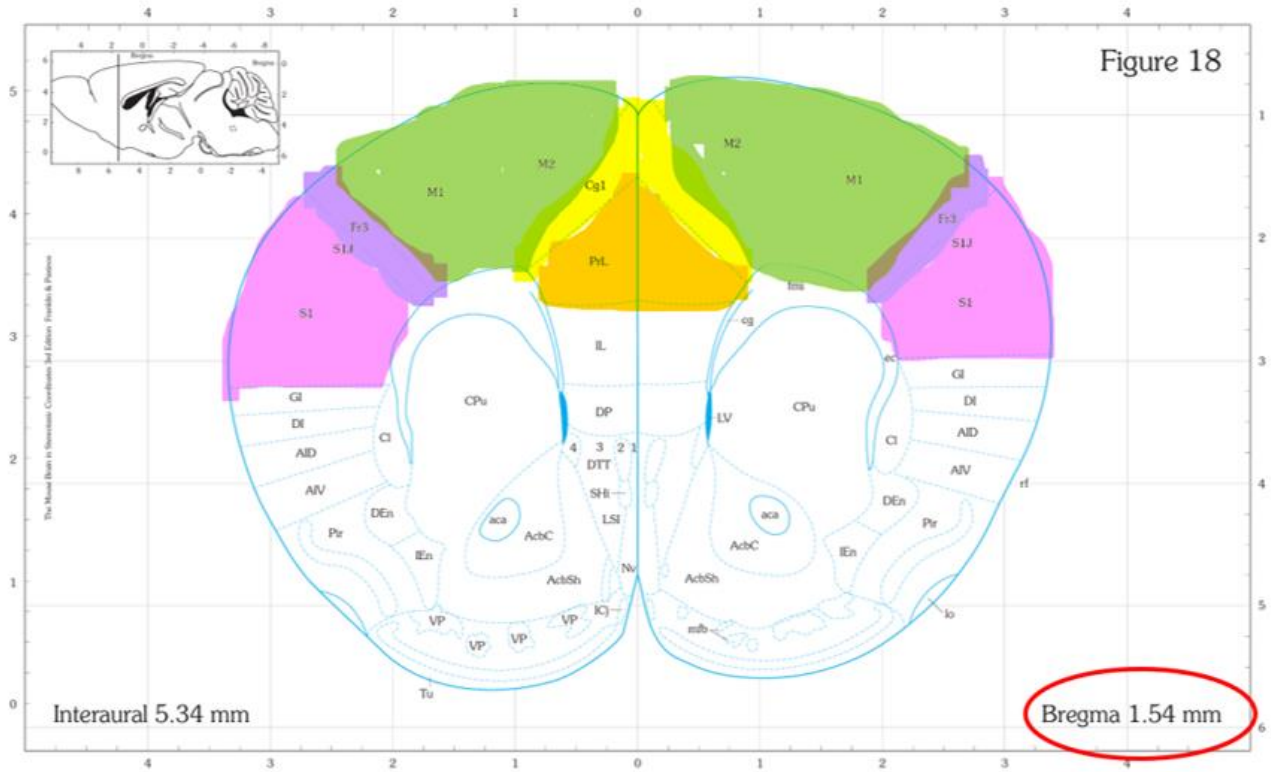
The Mouse Brain Atlas in Stereotaxic Coordinates  
 (Franklin Paxinos 3rd edition 2007 Elsevier Inc)

**Table A-1**

<b>Abbreviations</b>	<b>Regions of Interest Selected for Imaging</b>
<b>Cg1</b>	cingulate cortex, area 1
<b>M1</b>	primary motor cortex
<b>M2</b>	secondary motor cortex
<b>PrL</b>	prelimbic cortex
<b>RegFS</b>	frontal cortex, area 3 primary somatosensory cortex, jaw region
<b>RSD</b>	retrosplenial dysgranular cortex
<b>RSGc</b>	retrosplenial granular cortex, c region
<b>S1</b>	primary somatosensory cortex, forelimb region primary somatosensory cortex, jaw region primary somatosensory cortex, upper lip region primary somatosensory cortex, dysgranular zone secondary somatosensory cortex

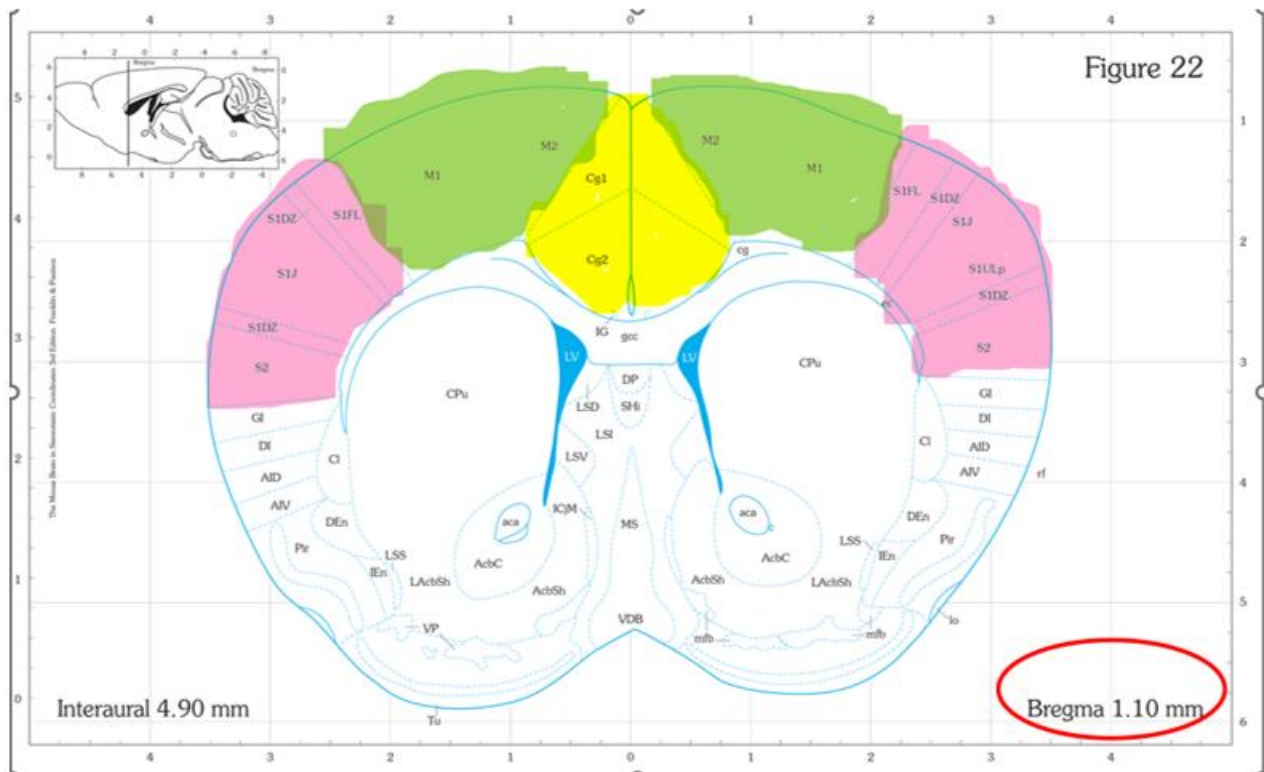
## Mouse Coronal Sections Used as References

**Figure A-1i**



- Cg1**    cingulate cortex, area 1
- PrL**    preLimbic
- FR3**    frontal cortex, area 3
- M1**    primary motor cortex
- M2**    secondary motor cortex
- S1**    primary somatosensory cortex
- S1J**    primary somatosensory cortex, jaw region

**Figure A-1ii**



- Cg1** cingulate cortex, area 1
- Cg2** cingulate cortex, area 2
- M1** primary motor cortex
- M2** secondary motor cortex
- S1** primary somatosensory cortex
- S2** secondary somatosensory cortex
- S1DZ** primary somatosensory cortex, dysgranular zone
- S1FL** primary somatosensory cortex, forelimb region
- S1J** primary somatosensory cortex, jaw region
- SIUL** primary somatosensory cortex upper lip
- SIULp** primary somatosensory cortex, upper lip region

## Total Images Collected

**Table A-2i**

Brain #	Type	Sex	Age	Total Sections	<u>PreLimbic</u>	Cg1	M2	M1	RegFS	<u>RegS</u>	RSD	RSGc	Total Images
31	WT	M	P31	6	41	30	45	88	0	76	16	17	313
36	WT	M	P28	6	0	23	54	73	48	64	6	23	299
35	16p11.2	M	P28	5	0	28	27	60	0	59	0	0	199
30	16p11.2	M	P31	5	0	27	20	43	0	101	0	0	208
37	16p11.2	F	P17	3	37	32	36	70	64	64	0	0	319
39	16p11.2	M	P17	6	23	37	56	99	36	83	0	0	354
Total					101	177	238	433	148	447	22	40	1692

Note total sections represent the number of 30  $\mu$ M that were used per mouse brain.

## Total Images Analyzed

**Table A-2ii**

Brain Region	Total Images Analyzed
Cg1	146
M1	405
M2	228
PrL	68
RegFS	146
RSD	22
RSGc	22
S1	247
<b>Total</b>	1284

## Appendix B Pipeline Workflow

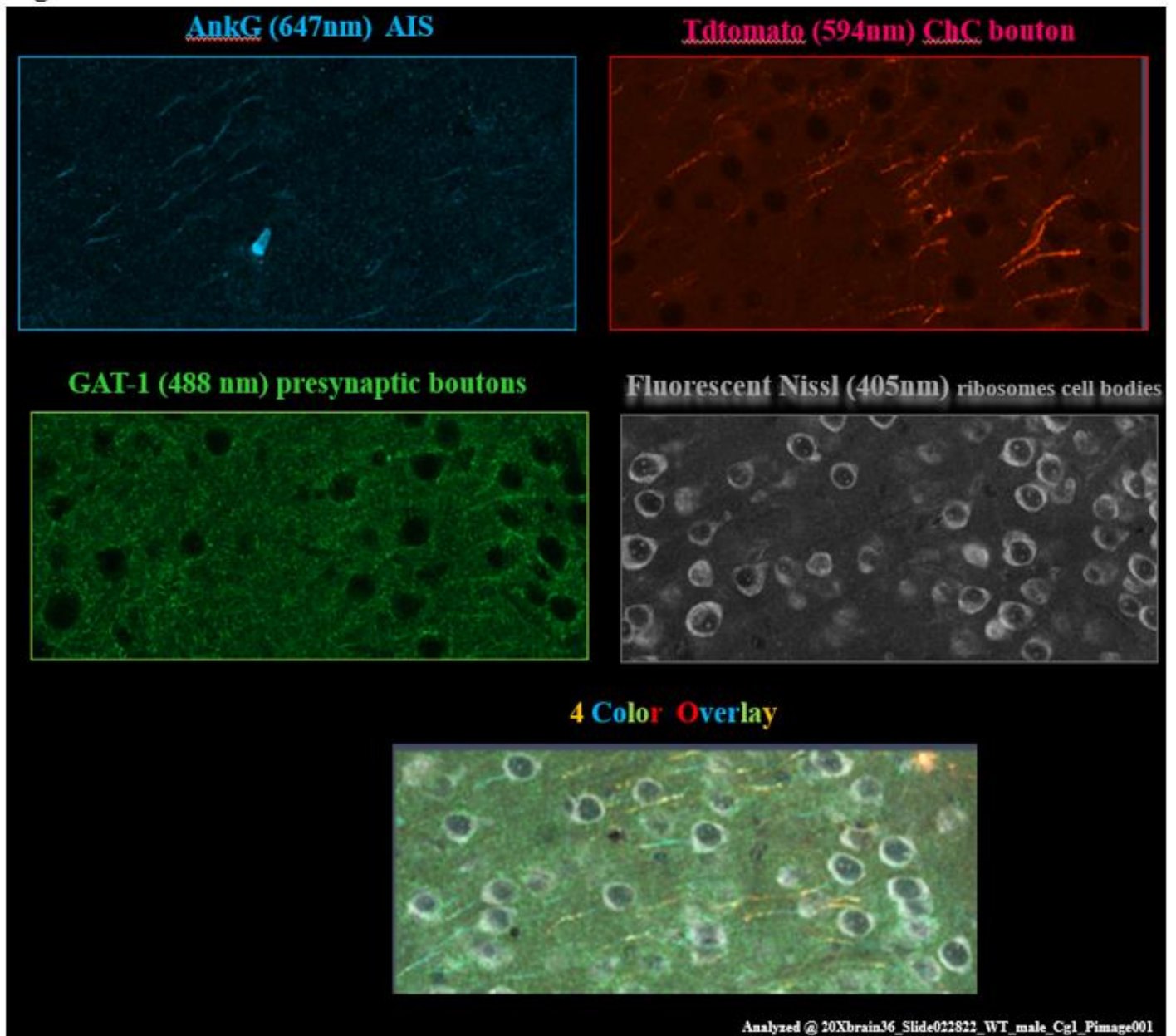
Confocal microscopy software: Zen 3.2 blue edition 2020 ©Carl Zeiss Microscopy GmbH

Figure B-1i



Figure -B1i: Utilized 4 channels to visualize the immunostained area of the neuron

**Figure B-1ii**



**Figure -B1i:** Example of image output from each of the 4 channels and the combined channel overlay



CellProfiler™ v4.2.1 cell imaging analysis software, Broad Institute  
The pipeline employed to analyze the data “AB ChC-bouto-counts-8.cproj”

Figure B-2

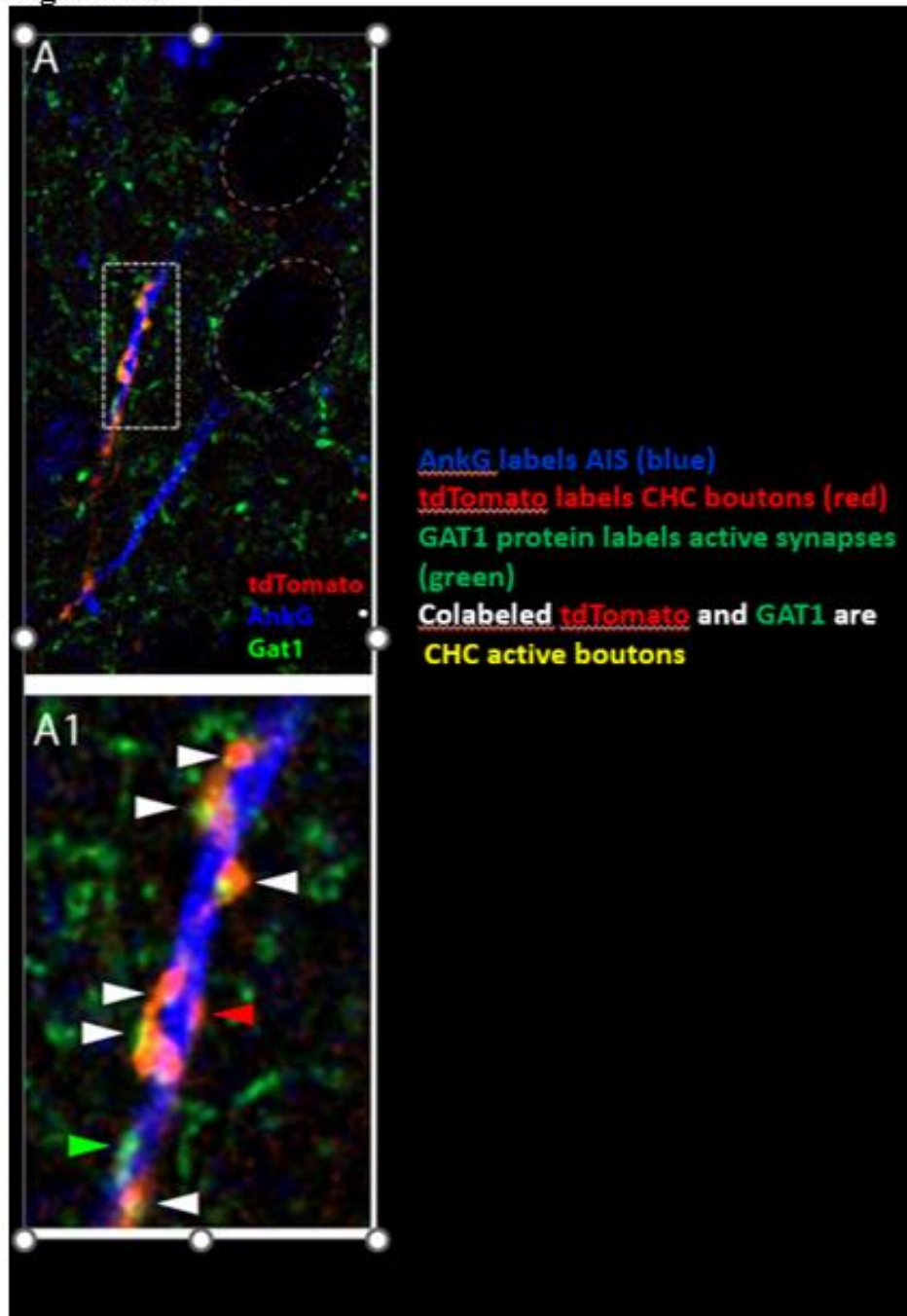


Figure B-2: Example of the fluorescent labeling of ChC bouton to the AIS of PyN

## References

- 1 Cheroni, C., Caporale, N. & Testa, G. Autism spectrum disorder at the crossroad between genes and environment: contributions, convergences, and interactions in ASD developmental pathophysiology. *Molecular Autism* 11, 1-18 (2020). <https://doi.org/doi:10.1186/s13229-020-00370-1>
- 2 Consortium, S. V. Simons Variation in Individuals Project (Simons VIP): A Genetics-First Approach to Studying Autism Spectrum and Related Neurodevelopmental Disorders. *Neuron* 73, 1063-1067 (2012). <https://doi.org/10.1016/j.neuron.2012.02.014>
- 3 Elsabbagh, M. *et al.* Global Prevalence of Autism and Other Pervasive Developmental Disorders. *Autism Research* 5, 160-179 (2012). <https://doi.org/10.1002/aur.239>
- 4 Government, C. f. D. C. U. Prevalence of Autism Spectrum Disorder Among Children Aged 8 Years — Autism and Developmental Disabilities Monitoring Network, 11 Sites, United States, 2016 | MMWR. (@CDCMMWR, 2020).
- 5 Zeidan, J. *et al.* Global prevalence of autism: A systematic review update. *Autism Research* 15, 778-790 (2022). <https://doi.org/10.1002/aur.2696>
- 6 Sharma, S., Gonda, X. & Tarazi, F. Autism Spectrum Disorder: Classification, diagnosis and therapy. *Pharmacology & Therapeutics* 190, 91-104 (2018). <https://doi.org/10.1016/j.pharmthera.2018.05.007>
- 7 Kanner, L. Autistic disturbances of affective contact. *Nervous child* 2, 217-250 (1943).
- 8 Association, A. P. *Diagnostic and Statistical Manual of Mental Disorders*. 5th edition edn, (2013).
- 9 Organization, W. h. *ICD-10: International Statistical Classification of Diseases and Related Health Problems: Tenth Revision*. 10 edn, Vol. 2 (WHO Library Cataloguing, 2004).
- 10 Hyman, S. L. *et al.* Identification, Evaluation, and Management of Children With Autism Spectrum Disorder. *Pediatrics* 145 (2022). <https://doi.org/10.1542/peds.2019-3447>
- 11 de Giambattista, C., Ventura, P., Trerotoli, P., Margari, F. & Margari, L. Sex Differences in Autism Spectrum Disorder: Focus on High Functioning Children and Adolescents. *Frontiers in Psychiatry* 12 (2021). <https://doi.org/10.3389/fpsy.2021.539835>
- 12 Sundaram, S. K. *et al.* Diffusion Tensor Imaging of Frontal Lobe in Autism Spectrum Disorder. *Cerebral Cortex* 18, 2659-2665 (2008). <https://doi.org/10.1093/cercor/bhn031>
- 13 Haar, S. *et al.* Anatomical Abnormalities in Autism? *Cerebral Cortex* 26, 1440-1452 (2016). <https://doi.org/10.1093/cercor/bhu242>
- 14 Chaste, P., Roeder, K., Devlin, B., Chakravarti, A. & Green, E. The Yin and Yang of Autism Genetics: How Rare De Novo and Common Variations Affect Liability. *Annual Review of Genomics and Human Genetics, Vol 18* 18, 167-187 (2017). <https://doi.org/10.1146/annurev-genom-083115-022647>
- 15 al., M. I. e. Pleiotropic Mechanisms Indicated for Sex Differences in Autism | PLOS Genetics. *12* (2016). <https://doi.org/10.1371/journal.pgen.1006425>
- 16 Zhang, Y. *et al.* Genetic evidence of gender difference in autism spectrum disorder supports the female-protective effect. *Translational Psychiatry* 10, 1-10 (2020). <https://doi.org/doi:10.1038/s41398-020-0699-8>
- 17 Berg, J. M. & Geschwind, D. H. Autism genetics: searching for specificity and convergence. *Genome Biology* 13, 1-16 (2012). <https://doi.org/doi:10.1186/gb-2012-13-7-247>



- 18 Wu, S. *et al.* Advanced parental age and autism risk in children: a systematic review and meta-analysis. *Acta Psychiatrica Scandinavica* 135, 29-41 (2017).  
<https://doi.org/10.1111/acps.12666>
- 19 Liu, F. *et al.* Altered composition and function of intestinal microbiota in autism spectrum disorders: a systematic review. *Translational Psychiatry* 9, 1-13 (2019).  
<https://doi.org/doi:10.1038/s41398-019-0389-6>
- 20 Sharon, G. *et al.* Human Gut Microbiota from Autism Spectrum Disorder Promote Behavioral Symptoms in Mice. *Cell* 177, 1600-+ (2019).  
<https://doi.org/10.1016/j.cell.2019.05.004>
- 21 Ronalds, A., a. H. R. Progress in Understanding the Causes of Autism Spectrum Disorders and Autistic Traits: Twin Studies from 1977 to the Present Day | SpringerLink. *Behavior Genetics of Psychopathology* (2014). [https://doi.org/10.1007/978-1-4614-9509-3\\_2](https://doi.org/10.1007/978-1-4614-9509-3_2)
- 22 O’Roak, B. J. *et al.* Sporadic autism exomes reveal a highly interconnected protein network of de novo mutations. *Nature* 485, 246-250 (2012).  
<https://doi.org/doi:10.1038/nature10989>
- 23 Chaste, P. *et al.* Adjusting Head Circumference for Covariates in Autism: Clinical Correlates of a Highly Heritable Continuous Trait. *Biological Psychiatry* 74, 576-584 (2013). <https://doi.org/10.1016/j.biopsych.2013.04.018>
- 24 Folstein, S. & Rutter, M. Genetic Influences And Infantile-Autism. *Nature* 265, 726-728 (1977). <https://doi.org/10.1038/265726a0>
- 25 al, T. B. e. Heritability of autism spectrum disorders: a meta-analysis of twin studies. *The Journal of Child Psychology and Psychiatry* (2015). <https://doi.org/10.1111/jcpp.12499>
- 26 Willsey, H. R., Willsey, A. J., Wang, B. & State, M. W. Genomics, convergent neuroscience and progress in understanding autism spectrum disorder. *Nature Reviews Neuroscience*, 1-19 (2022). <https://doi.org/doi:10.1038/s41583-022-00576-7>
- 27 Sherman, M. A. *et al.* Large mosaic copy number variations confer autism risk. *Nature Neuroscience* 24, 197-203 (2021). <https://doi.org/doi:10.1038/s41593-020-00766-5>
- 28 Vicari, S. *et al.* Copy number variants in autism spectrum disorders. *Progress in Neuro-Psychopharmacology & Biological Psychiatry* 92, 421-427 (2019).  
<https://doi.org/10.1016/j.pnpbp.2019.02.012>
- 29 Fischbach, G. & Lord, C. The Simons Simplex Collection: A Resource for Identification of Autism Genetic Risk Factors. *Neuron* 68, 192-195 (2010).  
<https://doi.org/10.1016/j.neuron.2010.10.006>
- 30 Hashem, S. *et al.* Genetics of structural and functional brain changes in autism spectrum disorder. *Translational Psychiatry* 10 (2020). <https://doi.org/10.1038/s41398-020-00921-3>
- 31 Takumi, T. & Tamada, K. CNV biology in neurodevelopmental disorders. *Current Opinion in Neurobiology* 48, 183-192 (2018). <https://doi.org/10.1016/j.conb.2017.12.004>
- 32 Carvalho, C. M. B. & Lupski, J. R. Mechanisms underlying structural variant formation in genomic disorders. *Nature Reviews Genetics* 17, 224-238 (2016).  
<https://doi.org/doi:10.1038/nrg.2015.25>
- 33 Sztainberg, Y. & Zoghbi, H. Y. Lessons learned from studying syndromic autism spectrum disorders. *Nature Neuroscience* 19, 1408-1417 (2016).  
<https://doi.org/doi:10.1038/nn.4420>

- 34 Hull, J. *et al.* Resting-State Functional Connectivity in Autism Spectrum Disorders: A Review. *Frontiers in Psychiatry* 7 (2017). <https://doi.org:10.3389/fpsy.2016.00205>
- 35 Wegiel, J. *et al.* The neuropathology of autism: defects of neurogenesis and neuronal migration, and dysplastic changes. *Acta Neuropathologica* 119, 755-770 (2010). <https://doi.org:doi:10.1007/s00401-010-0655-4>
- 36 Bedford, S. A. *et al.* Large-scale analyses of the relationship between sex, age and intelligence quotient heterogeneity and cortical morphometry in autism spectrum disorder. *Molecular Psychiatry* 25, 614-628 (2019). <https://doi.org:doi:10.1038/s41380-019-0420-6>
- 37 Varghese, M. *et al.* Autism spectrum disorder: neuropathology and animal models. *Acta Neuropathologica* 134, 537-566 (2017). <https://doi.org:doi:10.1007/s00401-017-1736-4>
- 38 Babaeeghazvini, P., Rueda-Delgado, L., Gooijers, J., Swinnen, S. & Daffertshofer, A. Brain Structural and Functional Connectivity: A Review of Combined Works of Diffusion Magnetic Resonance Imaging and Electro-Encephalography. *Frontiers in Human Neuroscience* 15 (2021). <https://doi.org:10.3389/fnhum.2021.721206>
- 39 Haghghat, H., Mirzarezaee, M., Araabi, B. N. & Khadem, A. Functional Networks Abnormalities in Autism Spectrum Disorder: Age-Related Hypo and Hyper Connectivity. *Brain Topography* 34, 306-322 (2021). <https://doi.org:doi:10.1007/s10548-021-00831-7>
- 40 Molyneaux, B. J., Arlotta, P., Menezes, J. R. L. & Macklis, J. D. Neuronal subtype specification in the cerebral cortex. *Nature Reviews Neuroscience* 8, 427-437 (2007). <https://doi.org:doi:10.1038/nrn2151>
- 41 Markram, H. *et al.* Interneurons of the neocortical inhibitory system. *Nature Reviews Neuroscience* 5, 793-807 (2004). <https://doi.org:doi:10.1038/nrn1519>
- 42 Cossart, R. & Garel, S. Step by step: cells with multiple functions in cortical circuit assembly. *Nature Reviews Neuroscience*, 1-16 (2022). <https://doi.org:doi:10.1038/s41583-022-00585-6>
- 43 Lim, L., Mi, D., Llorca, A. & Marin, O. Development and Functional Diversification of Cortical Interneurons. *Neuron* 100, 294-313 (2018). <https://doi.org:10.1016/j.neuron.2018.10.009>
- 44 Rudy, B., Fishell, G., Lee, S. & Hjerling-Leffler, J. Three Groups of Interneurons Account for Nearly 100% of Neocortical GABAergic Neurons. *Developmental Neurobiology* 71, 45-61 (2011). <https://doi.org:10.1002/dneu.20853>
- 45 Tau, G. Z. & Peterson, B. S. Normal Development of Brain Circuits. *Neuropsychopharmacology* 35, 147-168 (2009). <https://doi.org:doi:10.1038/npp.2009.115>
- 46 Antoine, M., Langberg, T., Schnepel, P. & Feldman, D. Increased Excitation-Inhibition Ratio Stabilizes Synapse and Circuit Excitability in Four Autism Mouse Models. *Neuron* 101, 648-+ (2019). <https://doi.org:10.1016/j.neuron.2018.12.026>
- 47 Velmeshev, D. *et al.* Cell-Type-Specific Analysis of Molecular Pathology in Autism Identifies Common Genes and Pathways Affected Across Neocortical Regions. *Molecular Neurobiology* 57, 2279-2289 (2020). <https://doi.org:10.1007/s12035-020-01879-5>
- 48 J., S. Module-Concept In Cerebral-Cortex Architecture. *Brain Research* 95, 475-496 (1975). [https://doi.org:10.1016/0006-8993\(75\)90122-5](https://doi.org:10.1016/0006-8993(75)90122-5)
- 49 Inan, M. & Anderson, S. The chandelier cell, form and function. *Current Opinion in Neurobiology* 26, 142-148 (2014). <https://doi.org:10.1016/j.conb.2014.01.009>

- 50 .D.A., L. The chandelier neuron in schizophrenia. *Developmental Neurobiology* 71, 118-  
127 (2011). <https://doi.org:10.1002/dneu.20825>
- 51 Marín, O. Interneuron dysfunction in psychiatric disorders. *Nature Reviews Neuroscience*  
13, 107-120 (2012). <https://doi.org:doi:10.1038/nrn3155>
- 52 Gallo, N., Paul, A. & Van Aelst, L. Shedding Light on Chandelier Cell Development,  
Connectivity, and Contribution to Neural Disorders. *Trends in Neurosciences* 43, 565-  
580 (2020). <https://doi.org:10.1016/j.tins.2020.05.003>
- 53 Wang, Y., Zhang, P. & Wyskiel, D. Chandelier Cells in Functional and Dysfunctional  
Neural Circuits. *Frontiers in Neural Circuits* 10 (2016).  
<https://doi.org:10.3389/fncir.2016.00033>
- 54 Ango, F., Gallo, N. & Van Aelst, L. Molecular mechanisms of axo-axonic innervation.  
*Current Opinion in Neurobiology* 69, 105-112 (2021).  
<https://doi.org:10.1016/j.conb.2021.03.002>
- 55 Tai .Y. et al. Regulation of Chandelier Cell Cartridge and Bouton Development via  
DOCK7-Mediated ErbB4 Activation. *Cell Reports* 6, 254-263 (2014).
- 56 Nahar, L., Delacroix, B. M. & Nam, H. W. The Role of Parvalbumin Interneurons in  
Neurotransmitter Balance and Neurological Disease. *Frontiers in Psychiatry* 12 (2021).  
<https://doi.org:10.3389/fpsy.2021.679960>
- 57 Schoenemann, P., Sheehan, M. & Glotzer, L. Prefrontal white matter volume is  
disproportionately larger in humans than in other primates. *Nature Neuroscience* 8, 242-  
252 (2005). <https://doi.org:10.1038/nn1394>
- 58 Bauman, M. & Schumann, C. Advances in nonhuman primate models of autism:  
Integrating neuroscience and behavior. *Experimental Neurology* 299, 252-265 (2018).  
<https://doi.org:10.1016/j.expneurol.2017.07.021>
- 59 Zaslavsky, K. *et al.* SHANK2 mutations associated with autism spectrum disorder cause  
hyperconnectivity of human neurons. *Nature Neuroscience* 22, 556-564 (2019).  
<https://doi.org:doi:10.1038/s41593-019-0365-8>
- 60 Urresti, J. *et al.* Cortical organoids model early brain development disrupted by 16p11.2  
copy number variants in autism. *Molecular Psychiatry* 26, 7560-7580 (2021).  
<https://doi.org:doi:10.1038/s41380-021-01243-6>
- 61 Iyer, J. *et al.* Pervasive genetic interactions modulate neurodevelopmental defects of the  
autism-associated 16p11.2 deletion in *Drosophila melanogaster*. *Nature Communications*  
9, 1-19 (2018). <https://doi.org:doi:10.1038/s41467-018-04882-6>
- 62 Blaker-Lee, A. *et al.* Zebrafish homologs of genes within 16p11.2, a genomic region  
associated with brain disorders, are active during brain development, and include two  
deletion dosage sensor genes. *Disease Models & Mechanisms* 5, 834-851 (2012).  
<https://doi.org:10.1242/dmm.009944>
- 63 Netser, S. *et al.* Distinct dynamics of social motivation drive differential social behavior  
in laboratory rat and mouse strains. *Nature Communications* 11, 1-19 (2020).  
<https://doi.org:doi:10.1038/s41467-020-19569-0>
- 64 Eberl, C. *et al.* Reproducible Colonization of Germ-Free Mice With the Oligo-Mouse-  
Microbiota in Different Animal Facilities. *Frontiers in Microbiology* 10 (2020).  
<https://doi.org:10.3389/fmicb.2019.02999>
- 65 Chung, W., Roberts, T., Sherr, E., Snyder, L. & Spiro, J. 16p11.2 deletion syndrome.  
*Current Opinion in Genetics & Development* 68, 49-56 (2021).  
<https://doi.org:10.1016/j.gde.2021.01.011>

- 66 Horev, G. *et al.* Dosage-dependent phenotypes in models of 16p11.2 lesions found in autism. *Proceedings of the National Academy of Sciences of the United States of America* 108, 17076-17081 (2011). <https://doi.org:10.1073/pnas.1114042108>
- 67 Rein, B. & Yan, Z. 16P11.2 Copy Number Variations and Neurodevelopmental Disorders. *Trends in Neurosciences* 43, 886-901 (2020).  
<https://doi.org:10.1016/j.tins.2020.09.001>
- 68 Green Snyder, L. *et al.* Autism Spectrum Disorder, Developmental and Psychiatric Features in 16p11.2 Duplication. *Journal of Autism and Developmental Disorders* 46, 2734-2748 (2016). <https://doi.org:doi:10.1007/s10803-016-2807-4>
- 69 Crepel, A. *et al.* Narrowing the Critical Deletion Region for Autism Spectrum Disorders on 16p11.2. *American Journal of Medical Genetics Part B-Neuropsychiatric Genetics* 156B, 243-245 (2011). <https://doi.org:10.1002/ajmg.b.31163>
- 70 Ip, J. *et al.* Major Vault Protein, a Candidate Gene in 16p11.2 Microdeletion Syndrome, Is Required for the Homeostatic Regulation of Visual Cortical Plasticity. *Journal of Neuroscience* 38, 3890-3900 (2018). <https://doi.org:10.1523/JNEUROSCI.2034-17.2018>
- 71 Frazier, T. Autism Spectrum Disorder Associated with Germline Heterozygous PTEN Mutations. *Cold Spring Harbor Perspectives in Medicine* 9 (2019).  
<https://doi.org:10.1101/cshperspect.a037002>
- 72 Escamilla, C. O. *et al.* Kctd13 deletion reduces synaptic transmission via increased RhoA. *Nature* 551, 227-231 (2017). <https://doi.org:doi:10.1038/nature24470>
- 73 Calderon de Anda, F. *et al.* Autism spectrum disorder susceptibility gene TAOK2 affects basal dendrite formation in the neocortex. *Nature Neuroscience* 15, 1022-1031 (2012).  
<https://doi.org:doi:10.1038/nn.3141>
- 74 Shen, Y. *et al.* Intra-Family Phenotypic Heterogeneity of 16p11.2 Deletion Carriers in a Three-Generation Chinese Family. *American Journal of Medical Genetics Part B-Neuropsychiatric Genetics* 156B, 225-232 (2011). <https://doi.org:10.1002/ajmg.b.31147>
- 75 Kumar, A. *et al.* Alterations in Frontal Lobe Tracts and Corpus Callosum in Young Children with Autism Spectrum Disorder. *Cerebral Cortex* 20, 2103-2113 (2009).  
<https://doi.org:10.1093/cercor/bhp278>
- 76 Tai, Y., Gallo, N., Wang, M., Yu, J. & Van Aelst, L. Axo-axonic Innervation of Neocortical Pyramidal Neurons by GABAergic Chandelier Cells Requires AnkyrinG-Associated L1CAM. *Neuron* 102, 358-+ (2019).  
<https://doi.org:10.1016/j.neuron.2019.02.009>
- 77 Ariza, J., Rogers, H., Hashemi, E., Noctor, S. & Martinez-Cerdeno, V. The Number of Chandelier and Basket Cells Are Differentially Decreased in Prefrontal Cortex in Autism. *Cerebral Cortex* 28, 411-420 (2018). <https://doi.org:10.1093/cercor/bhw349>
- 78 Amina, S. *et al.* Chandelier Cartridge Density Is Reduced in the Prefrontal Cortex in Autism. *Cerebral Cortex* 31, 2944-2951 (2021). <https://doi.org:10.1093/cercor/bhaa402>
- 79 Bertero, A. *et al.* Autism-associated 16p11.2 microdeletion impairs prefrontal functional connectivity in mouse and human. *Brain* 141, 2055-2065 (2018).  
<https://doi.org:10.1093/brain/awy111>
- 80 Paul, A. *et al.* Transcriptional Architecture of Synaptic Communication Delineates GABAergic Neuron Identity. *Cell* 171, 522-+ (2017).  
<https://doi.org:10.1016/j.cell.2017.08.032>
- 81 al., M. C. e. CellProfiler 3.0: Next-generation image processing for biology. (2018).  
<https://doi.org:10.1371/journal.pbio.2005970>

- 82 JASP (Version 0.16.2)[Computer software] v. Version 0.16.2 [Computer software]  
(@MISC {JASP2022}, 2022).
- 83 Harris, K. & Stevens, J. Dendritic Spines Of Ca-1 Pyramidal Cells In The Rat  
Hippocampus - Serial Electron-Microscopy With Reference To Their Biophysical  
Characteristics. *Journal of Neuroscience* 9, 2982-2997 (1989).
- 84 Murthy, V. N., Schikorski, T., Stevens, C. F. & Zhu, Y. Inactivity produces increases in  
neurotransmitter release and synapse size. *Neuron* 32, 673-682 (2001).  
[https://doi.org:10.1016/s0896-6273\(01\)00500-1](https://doi.org:10.1016/s0896-6273(01)00500-1)
- 85 Hofer, S. B., Mrsic-Flogel, T. D., Bonhoeffer, T. & Hübener, M. Experience leaves a  
lasting structural trace in cortical circuits. *Nature* 457, 313-317 (2009).  
<https://doi.org:10.1038/nature07487>
- 86 Kasai, H., Fukuda, M., Watanabe, S., Hayashi-Takagi, A. & Noguchi, J. Structural  
dynamics of dendritic spines in memory and cognition. *Trends Neurosci* 33, 121-129  
(2010). <https://doi.org:10.1016/j.tins.2010.01.001>
- 87 Ruediger, S. *et al.* Learning-related feedforward inhibitory connectivity growth required  
for memory precision. *Nature* 473, 514-518 (2011). <https://doi.org:10.1038/nature09946>
- 88 Marik, S. A., Yamahachi, H., McManus, J. N., Szabo, G. & Gilbert, C. D. Axonal  
dynamics of excitatory and inhibitory neurons in somatosensory cortex. *PLoS Biol* 8,  
e1000395 (2010). <https://doi.org:10.1371/journal.pbio.1000395>
- 89 Isabel del Pino and Cristina García-Frigola and Nathalie Dehorter and Jorge , R. B.-M. a.  
E. A.-S. a. M. Martínez de L. a. G. C. a. María V. Erbb4 Deletion from Fast-Spiking  
Interneurons Causes Schizophrenia-like Phenotypes. *Neuron* 79, 1152-1168 (2013).  
<https://doi.org:https://doi.org/10.1016/j.neuron.2013.07.010>
- 90 al., H. W. C. e. Social Behavior Is Modulated by Valence-Encoding mPFC-Amygdala  
Sub-circuitry. *Cell Reports* 32, 107899 (2020).  
<https://doi.org:https://doi.org/10.1016/j.celrep.2020.107899>
- 91 Lu, J. *et al.* Selective inhibitory control of pyramidal neuron ensembles and cortical  
subnetworks by chandelier cells. *Nature Neuroscience* 20, 1377-1383 (2017).  
<https://doi.org:doi:10.1038/nn.4624>
- 92 Balasco, L., Provenzano, G. & Bozzi, Y. Sensory Abnormalities in Autism Spectrum  
Disorders: A Focus on the Tactile Domain, From Genetic Mouse Models to the Clinic.  
*Frontiers in Psychiatry* 10 (2020). <https://doi.org:10.3389/fpsy.2019.01016>